AD_____

Award Number: W81XWH-09-1-0184

TITLE: Defining the Role of BTLA in Breast Cancer Immunosurveillance and Selective Targeting of the BTLA-HVEM-LIGHT Costimulatory System

PRINCIPAL INVESTIGATOR: William E. Gillanders, M.D.
Kenneth M. Murphy, M.D.

CONTRACTING ORGANIZATION:
Washington University
St. Louis, MO 63130-4862

REPORT DATE: May 2010

TYPE OF REPORT: Annual

PREPARED FOR: U.S. Army Medical Research and Materiel Command
Fort Detrick, Maryland 21702-5012

DISTRIBUTION STATEMENT:

× Approved for public release; distribution unlimited

# REPORT DOCUMENTATION PAGE

*Form Approved*
*OMB No. 0704-0188*



| **1. REPORT DATE** *(DD-MM-YYYY)* | **2. REPORT TYPE** | **3. DATES COVERED** *(From - To)* |
|---|---|---|
| 01-05-2010 | Annual | 1 MAY 2009 - 30 APR 2010 |

**4. TITLE AND SUBTITLE**
Defining the Role of BTLA in Breast Cancer Immunosurveillance and Selective Targeting of the BTLA-HVEM-LIGHT Costimulatory System

**5a. CONTRACT NUMBER**

**5b. GRANT NUMBER**
W81XWH-09-1-0184

**5c. PROGRAM ELEMENT NUMBER**

**6. AUTHOR(S)**
William Gillanders, Kenneth Murphy

**5d. PROJECT NUMBER**

**5e. TASK NUMBER**

**5f. WORK UNIT NUMBER**

**7. PERFORMING ORGANIZATION NAME(S) AND ADDRESS(ES)**
The Washington University
Saint Louis, MO 63130-4862

**8. PERFORMING ORGANIZATION REPORT NUMBER**

**9. SPONSORING / MONITORING AGENCY NAME(S) AND ADDRESS(ES)**
US Army Medical Research and Materiel Command
Fort Detrick, Maryland
21702-5012

**10. SPONSOR/MONITOR'S ACRONYM(S)**

**11. SPONSOR/MONITOR'S REPORT NUMBER(S)**

**12. DISTRIBUTION / AVAILABILITY STATEMENT**
Approved for public release; distribution unlimited

**13. SUPPLEMENTARY NOTES**

**14. ABSTRACT**
See attached

**15. SUBJECT TERMS**

| **16. SECURITY CLASSIFICATION OF:** | | | **17. LIMITATION OF ABSTRACT** | **18. NUMBER OF PAGES** | **19a. NAME OF RESPONSIBLE PERSON** |
|---|---|---|---|---|---|
| **a. REPORT** | **b. ABSTRACT** | **c. THIS PAGE** | | | USAMRMC |
| U | U | U | UU | 57 | **19b. TELEPHONE NUMBER** *(include area code)* |

**Standard Form 298 (Rev. 8-98)**
**Prescribed by ANSI Std. Z39.18**

## TABLE OF CONTENTS

## INTRODUCTION

**BACKGROUND:** In the last decade, considerable progress has been made in understanding the complex regulatory networks that control immune responses. Regulating the extent, quality and duration of immune responses is critical for balancing protective immunity and tissue injury. Costimulatory (CD28, ICOS) and inhibitory (CTLA4, PD-1) molecules of the CD28 receptor family provide critical secondary signals regulating this balance, and recent work has uncovered critical roles for CTLA4 and PD-1 in restraining immune responses in chronic viral infection and malignancy. We recently cloned B- and T-lymphocyte attenuator (BTLA), the third inhibitory receptor of the CD28 family expressed on lymphocytes. Using BTLA-deficient mice and monoclonal antibodies specific for BTLA that we generated, we have studied several in vivo models of infection and autoimmunity, showing the importance of BTLA in regulating immune responses. Several lines of evidence suggest that inhibitory molecules such as CTLA-4 and PD-1 limit cancer immunosurveillance.

**OBJECTIVE/HYPOTHESIS:** The hypothesis of this application is that BTLA contributes to the inhibition of breast cancer immunosurveillance, and selective targeting of the BTLA-LIGHT-HVEM costimulatory system can enhance breast cancer immunity.

**SPECIFIC AIMS:**

(1) Define the role of BTLA in breast cancer immunosurveillance.

(2) Determine if inhibitory molecules of the CD28 receptor family function as redundant immunologic checkpoints in breast cancer immunosurveillance.

(3) Develop novel therapeutics to successfully dissociate T cell costimulation and inhibition in the BTLA-LIGHT-HVEM costimulatory system.

**PROGRESS:** The award was in the format of a Synergistic Idea Award to William E. Gillanders, M.D., a breast cancer surgeon, and Kenneth Murphy, M.D., Ph.D., a basic immunologist. The current reporting period represents approximately the first year of a two year award. The overall aim is to evaluate the role of BTLA in breast cancer immunosurveillance, and develop novel therapeutics targeting the BTLA-LIGHT-HVEM costimulatory system. The research proposed relies heavily on genetically engineered mice that spontaneously develop breast cancer (BALB/c-neuT mice). These mice are currently being expanded and bred to gene-deficient mice to definitively evaluate the role of BTLA, CTLA4 and PD-1 in this process. Correlative studies are also underway using human tissue specimens. Although using genetically engineered mice that spontaneously develop breast cancer has a number of advantages, these studies require an initial investment in time to establish mice on the desired genetic background, and to establish cohorts of mice that will develop breast cancers at 25-30 weeks of age.

## BODY

**Specific Aims 1A, 1C, 2A, 2B:** The studies outlined in these Aims are underway. BALB/c-neuT mice are currently being bred to BTLA-deficient mice and PD-1-deficient mice. Cohorts of these mice are currently being established and will be evaluated when sufficient animals are available at the appropriate age (25-30 weeks). No spontaneous tumors from BALB/c-neuT mice have been evaluated to date as animals of sufficient age and appropriate genetic background are not yet available.

**Specific Aim 1B:** We have written a dedicated human studies protocol for the studies outlined in this Specific Aim. This human studies protocol was approved by the Siteman Cancer Center Protocol Review and Monitoring Committee and the Washington University School of Medicine Human Studies Committee. The protocol was also reviewed and approved by the U.S. Army Human Subjects Research Review Board. To date, biologic specimens have been obtained from six subjects, and these specimens have been processed and cryopreserved, and are ready for further analysis To facilitate the phenotypic analysis of tumor-infiltrating and peripheral blood lymphocytes, a protocol for multi-parametric flow cytometry was designed and validated. The protocol is based on identification of breast cancer-specific T cells through a combination of tetramer and CD8 antibody staining, followed by further assessment of phenotypic and functional markers. Please see Appendix # 1 for additional details. Please note that this flow cytometry protocol will also be used in Specific Aim 1 A when the mice are available.

**Specific Aim 3A:** The interaction between BTLA and HVEM is unique as no other interaction between molecules of the CD28 and TNF receptor families has been described. This unique interaction represents an exceptional opportunity to successfully develop novel therapeutics capable of dissociating T cell costimulation and inhibition. HVEM-mediated LIGHT signaling results in CD28-independent T cell costimulation, dramatically enhancing antitumor and other cell-mediated immune responses, whereas HVEM-mediated BTLA signaling induces inhibitory signals. We have successfully created three different HVEM mutants using site-directed mutagenesis: P17A, Y23A, and V36A with the goal to ablate HVEM interaction with BTLA but preserve HVEM interaction with LIGHT. The mutant constructs are being expressed in NIH 3T3 cells for further functional analysis. Please see Appendix #2 for additional details.

**Specific Aims 3B, 3C:** The experiments in these Specific Aims will be performed after *in vitro* validation of the constructs as outlined in Specific Aim 3A.

**Additional Studies:** Additional mechanistic of BTLA biology have been performed in the Murphy laboratory, pending availability of BALB/c-neuT mice of the appropriate age and genetic background. These studies of the BTLA-LIGHT-HVEM costimulatory system have been carried out in a murine model of graft-versus-host disease (see accompanying manuscript). Based upon the likely similarity of the mechanisms of action of BTLA in breast cancer-specific T cells and in expanding T cells in the GVHD model, we have carried out a series of studies into the mechanism and effects of BTLA-directed immunotherapy. In GVHD, T cells expanding

following bone marrow transplantation not only manifest graft-versus-host disease, but also mediate important antitumor effects. Therefore, we have carried out an analysis to evaluate the role of BTLA-directed therapy in this setting. The model used is the fully irradiated GVHD model. Two forms of this were tested, including a fully MHC-mismatched model of B6 transfer into BALB/c recipients, or a parental into F1 model. In both cases, either lethal or chronic GVHD is established, concurrent with significant weight loss, and a permanent mucosal inflammatory disease in the gut and elsewhere. Our essential finding is that the treatment of recipient mice with a single injection of anti-BTLA antibody (6A6) results in permanent prevention of GVHD. We find that treatment at the time of bone marrow transplantation (BMT) leads to a permanent cure, but that treatment with antibody delayed by 7 or 14 days fails to have any impact on the prevention of GVHD. In analyzing this observation, we have found that the effect is mediated by alteration of populations of T cells expanding during the period of lymphopenia immediately following BMT. The accompanying manuscript has been submitted to *Nature Immunology*, and has received favorable reviews with suggestions for additional experiments, which we are currently undertaking. In these additional experiments, we have used Foxp3-reportor mice in a series of cellular adoptive transfer experiments and have evaluated the effects of BTLA-directed therapy. The results indicate that BTLA acts on the expanding effector cells, exerting a preferential inhibition of their expansion compared to the expansion of regulatory T cells. This may relate to our earlier observations that effector cells express high levels of BTLA, whereas regulatory T cells express lower levels of BTLA and therefore may be inhibited to a lesser extent than expanding effector T cells. This prevention of robust effector cell expansion during lymphopenia following BMT may have the effect of limiting the expansion of auto-reactive T cells that are driven to expand through antigen interactions during the period of lymphopenia. By allowing the establishment of an appropriate balance between regulatory T cell populations and the effector cells that they control, a permanent cure and prevention of GVHD appears to take place once lymphopenic homeostatic expansion ceases in the recipient about 7-14 days following BMT. Of relevance to the current proposal, we have found that HVEM is not involved in the mechanisms of the beneficial effects of BTLA-directed therapy. During homeostatic expansion, HVEM is not engaged to limit the expansion of effector T cells after BMT. This observation may alter our future focus to concentrate on BTLA rather than HVEM manipulations in considering ways to augment anti-tumor vaccinations.

**Problem Areas:** We encountered an unforeseen problem when the postdoctoral fellow recruited to work specifically on this project left unexpectedly due to a family health issue, as covered under FMLA. This individual ultimately resigned the position. We have now successfully recruited another postdoctoral fellow to fill the position. This individual has a strong background in tumor immunology and vaccine development.

## KEY RESEARCH ACCOMPLISHMENTS

(1) Generation of proposed genetic strains is completed or underway.

(2) Successful initiation of human studies, with biologic specimens from six subjects obtained to date.

(3) Successful creation of HVEM mutants. These will be used as novel molecular adjuvants in a breast cancer DNA vaccine model.

(4) Identification of an effect of BTLA-directed therapy in the treatment of graft-versus-host disease, which may have relevance to breast cancer-specific T cells.

## REPORTABLE OUTCOMES

The accompanying manuscript has been submitted to *Nature Immunology* and is currently under revision. This unanticipated result was obtained during the period of time in which the major activities involved generation of various mouse strains.

## CONCLUSIONS

Progress has been made towards the goal of defining the role of BTLA in breast cancer immunosurveillance. Analysis of spontaneous breast cancers in mice of the appropriate age and genetic background will be required to complete the objectives of the proposal. Mechanistic studies in a model of GVHD confirm the importance of the BTLA-LIGHT-HVEM costimulatory system, and will help direct ongoing studies.

## APPENDICES

Appendix #1: Establishment of a validated multi-parametric flow cytometry protocol

Appendix #2: Generation of HVEM mutants

Appendix #3: Manuscript submitted to *Nature Immunology*

## Appendix 1: Establishment of a validated multi-parametric flow cytometry protocol

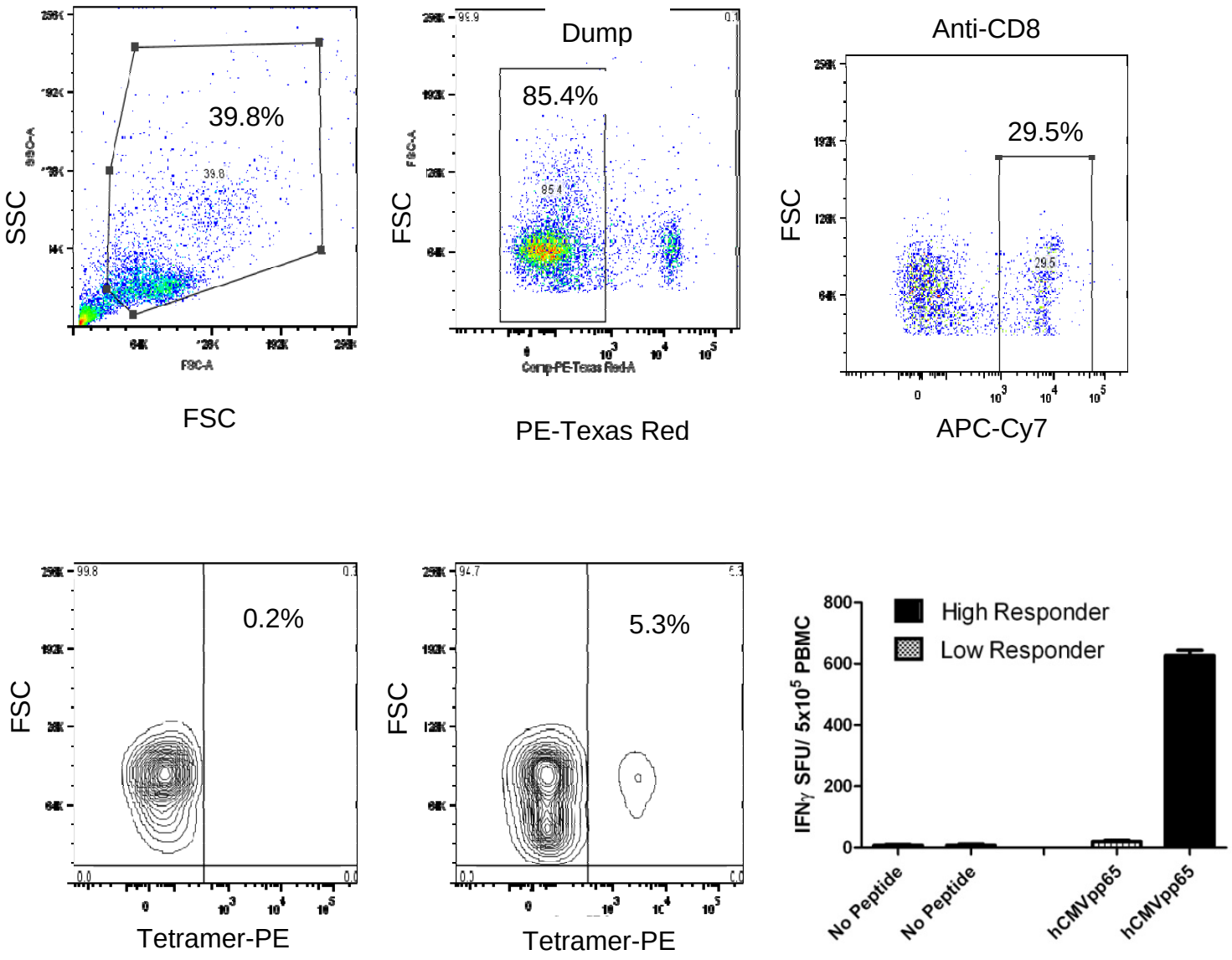


**Figure 1. hCMV-specific PBMC detected by multi-parametric flow cytometry and ELISPOT.** PBMC from a predetermined responder and non-responder to the hCMVpp65 peptide, NLVPMVAT were stained with the following fluorescently labeled antibodies: anti-CD8 APC-Cy7, anti-CD14 PE-Cy5, anti-CD19 PE-Cy5, anti-CD56 PE-Cy5, and CMVpp65 tetramer-PE. Optimal antibody concentrations were determined by titration of each antibody on PBMC (data not shown). Unstained PBMC, and PBMC stained with individual antibodies were used to set up compensation on the BD LSR II flow cytometer. Data were analyzed using FlowJo software (Treestar Inc, Ashland, OR). The percentage $CD8^+tetramer^+$ PBMC was determined by first selecting viable leucocytes (top left panel) based on forward scatter (FSC) and side scatter (SSC), followed by selection of CD14, CD19, and CD56-negative cells (dump gate, top middle panel). Next, CD8-positive cells were selected (top right panel). The percentage of CMV tetramer-positive cells was subsequently assessed within the CD8 fraction (bottom left and middle panels). The percent gated cells is displayed in each plot. Accordingly, the non-responder to hCMVpp65 contained 0.2% $CD8^+tetramer^+$ PBMC, and the high responder 5.3% $CD8^+tetramer^+$ PBMC. These data correlate with results from an IFN-γ ELISPOT assay using the same PBMC stimulated with the hCMV peptide (bottom right panel).

To more accurately establish compensation corrections for spectral overlap for any combination of fluorochrome-labeled antibodies, the BD™ CompBeads set was used to perform compensation settings for multicolor flow cytometry. The set consists of two populations of microparticles, the anti-mouse Ig, κ particles that bind any mouse κ light chain-bearing immunoglobulin, and the negative control (Fetal Bovine Serum) particles that have no binding capacity. When mixed together with a fluorochrome-conjugated mouse antibody, the BDTM CompBeads provide distinct positive and negative (background fluorescence) stained populations which can be used to set compensation levels. The compensation adjustments are made using the same fluorochrome-labeled antibody to be used in experiments, as shown for representative antibodies below: anti-CD14 -, anti-CD19 -, and anti-CD56-PerCP-Cy5.5 (dump channel), anti-CD3 Pacific Blue, and anti-CD8 APC-Cy7.

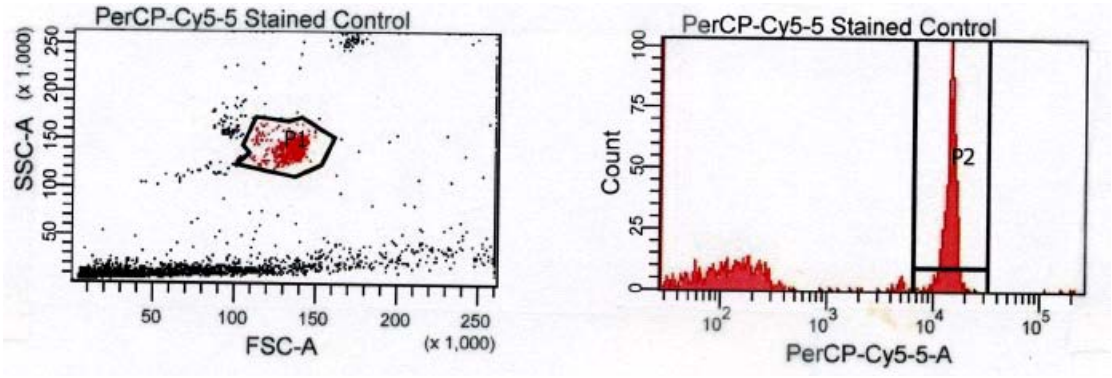


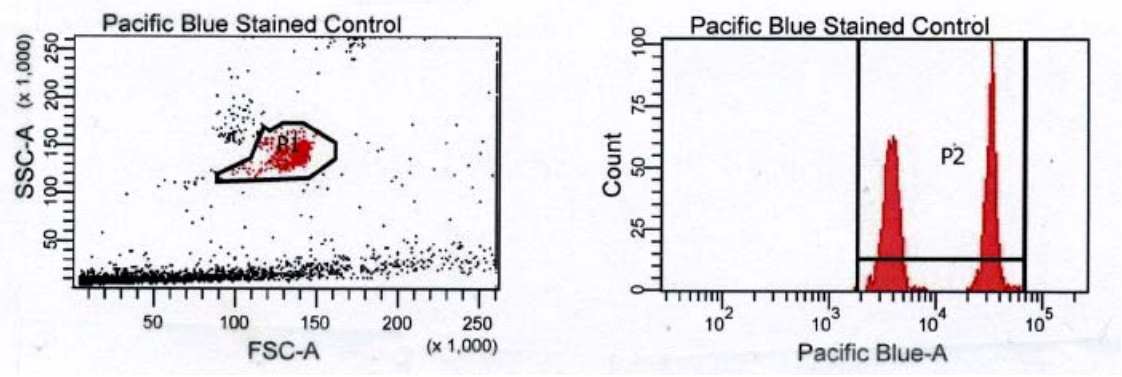


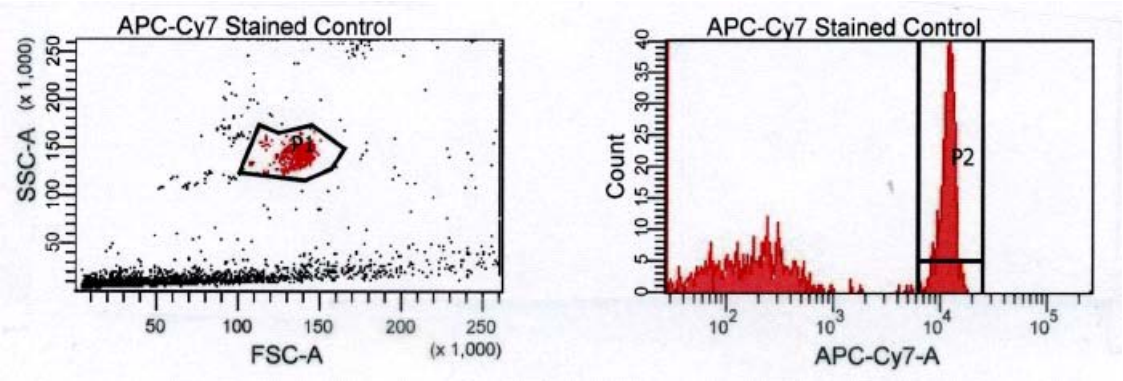

Peripheral blood mononuclear cells (PBMC) from a healthy donor were used for pilot experiments. Individual samples were prepared for each antibody, and the CompBeads set was added to all these samples. In addition, a sample was prepared containing all antibodies without the beads. The following antibodies were used: anti-CD3 Pacific Blue, anti-CD8 APC-Cy7, anti-CD14-, anti-CD19-, and anti-CD56-PE-Cy5.5, and anti-CD45RA-Qdot655. Samples were analyzed using FACSDiva Version 6.1.1 software. To assess the percentage of naïve CD8+ T cells in the PBMC, first PE Cy5.5-negative cells were selected (dump channel). Next, CD3+ (Pacific Blue) cells were positively selected, followed by selection of CD8+ cells (APC-Cy7). Lastly, the percentage of CD45RA-positive (Qdot-655) CD8 cells can be determined.

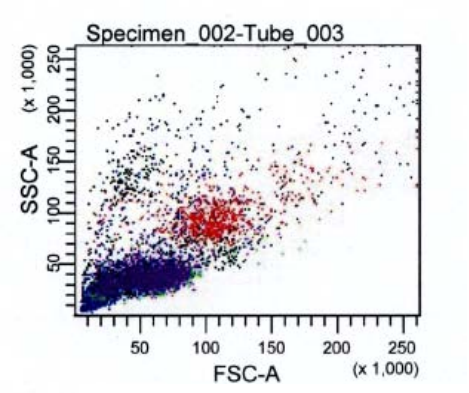


**Anti-CD14, CD19, CD56**

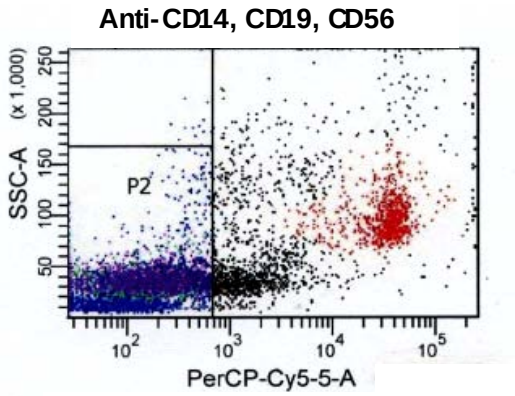


**Anti-CD3**

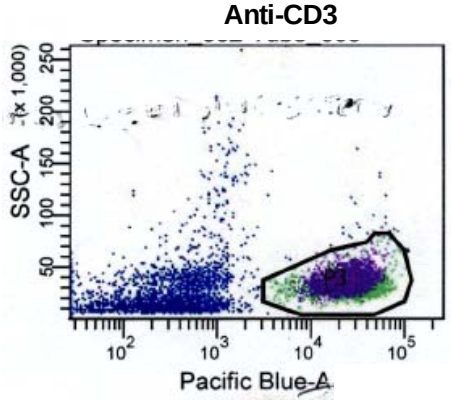


**Anti-CD8**

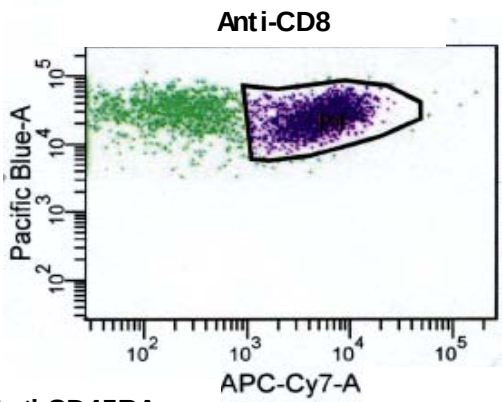


**Anti-CD45RA**

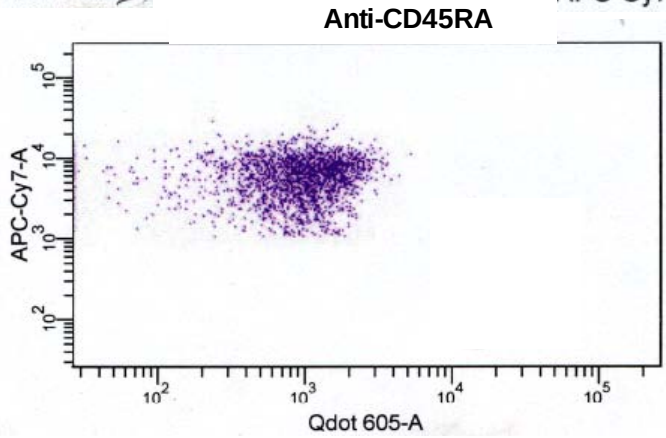


Tube: Tube_003

| Population | #Events | %Parent | %Total |
|---|---|---|---|
| All Events | 10,000 | #### | 100.0 |
| P1 | 727 | 7.3 | 7.3 |
| P2 | 7,829 | 78.3 | 78.3 |
| P3 | 3,692 | 47.2 | 36.9 |
| P4 | 2,023 | 54.8 | 20.2 |

## Appendix 2: Generation of HVEM mutants

Goal: Introduce three mutations into the HVEM-IRES-GFP-RV vector (P17A, Y23A, V36A)


**HVEM**

275 aa

HVEM-IRES-GFP-RV (7286 bp)

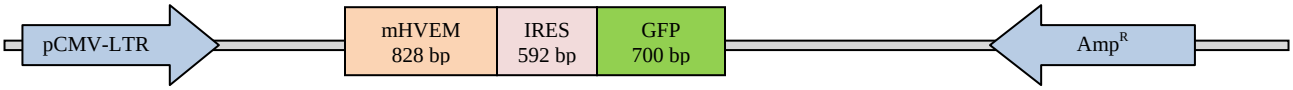


**HVEM SDM Primers**

```
mP17AFP GACGAGTGCTGCGCCATGTGCAACCCA
mP17ARP TGGGTTGCACATGGCGCAGCACTCGTC
mY23AFP GCAACCCAGGTGCCCATGTGAAGCAGG
mY23ARP CCTGCTTCACATGGGCACCTGGGTTGC
mV36AFP TACAGGCACAGCCTGTGCCCCCTGTCC
mV36ARP GGACAGGGGGCACAGGCTGTGCCTGTA
```

```
LOCUS       NM_178931               828 bp    mRNA    linear   ROD 15-JUN-2008
DEFINITION Mus musculus tumor necrosis factor receptor superfamily, member 14
           (herpesvirus entry mediator) (Tnfrsf14), mRNA.

  1 atggaacctc tcccaggatg ggggtcggca ccctggagcc aggcccctac agacaacacc
 61 ttcaggctgg tgccttgtgt cttccttttg aacttgctgc agcgcatctc tgcccagccc
121 tcatgcagac aggaggagtt ccttgtggga gacgagtgct gccccatgtg caacccaggt
181 taccatgtga agcaggtctg cagtgagcat acaggcacag tgtgtgcccc ctgtccccca
241 cagacatata ccgcccatgc aaatggcctg agcaagtgtc tgccctgcgg agtctgtgat
301 ccagacatgg gcctgctgac ctggcaggag tgctccagct ggaaggacac tgtgtgcaga
361 tgcatcccag gctacttctg tgagaaccag gatgggagcc actgttccac atgcttgcag
421 cacaccacct gccctccagg gcagagggta gagaagagag ggactcacga ccaggacact
481 gtatgtgctg actgcctaac agggaccttc tcacttggag ggactcagga ggaatgcctg
541 ccctggacca actgcagtgc atttcaacag gaagtaagac gtgggaccaa cagcacagac
601 accacctgct cctcccaggt cgtctactac gttgtgtcca tccttttgcc acttgtgata
661 gtgggagctg ggatagctgg attcctcatc tgcacgcgaa gacacctgca caccagctca
721 gtggccaagg agctggagcc tttccaggaa caacaggaga acaccatcag gtttccagtc
781 accgaggttg ggtttgctga gaccgaggag gagacagcct ccaactga
```

HVEM-IRES-GFP-RV (7286 bp)

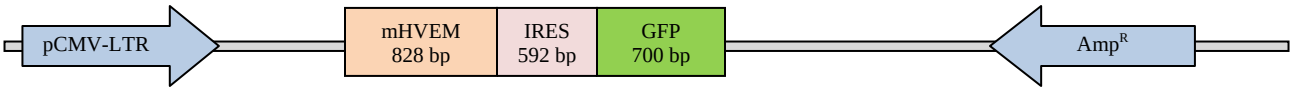

Use site-directed mutagenesis to insert mutations. Screen bacterial plates for presence of HVEM by restriction digest.

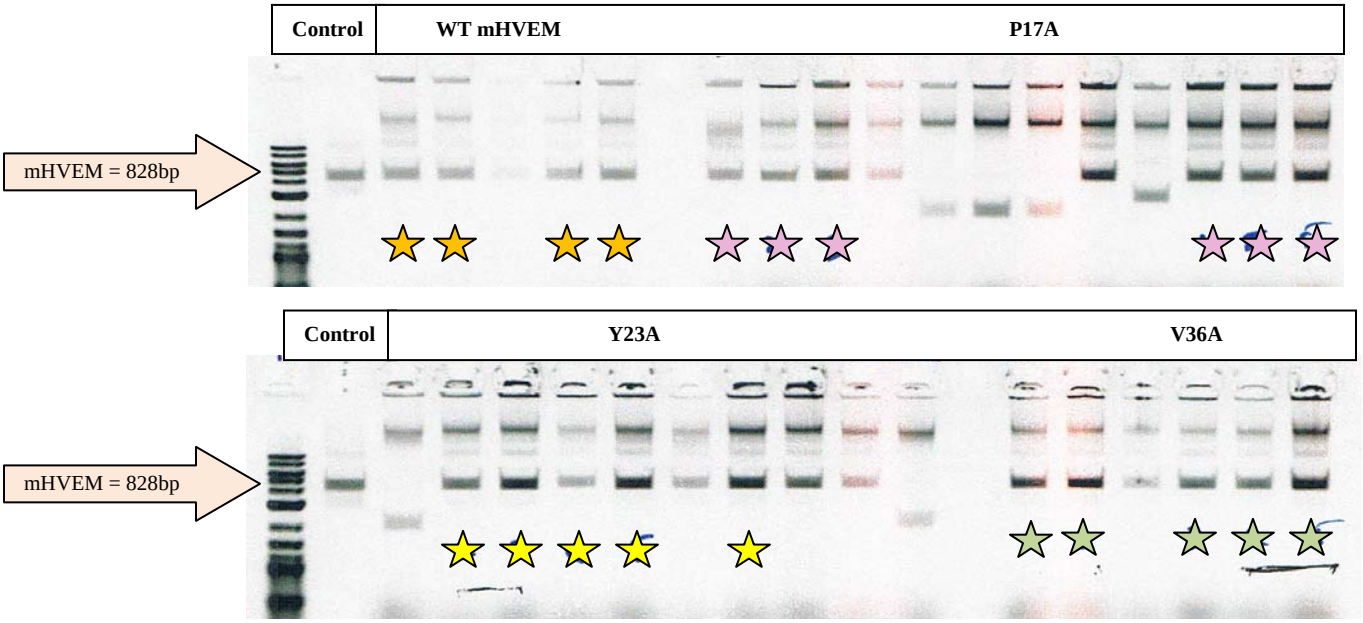


Constructs were positive by RE digest→ Indicated constructs were sent for sequencing to confirm mutations.

After positive sequencing reactions, constructs were midiprepped and DNA was prepared for virus packaging in Phoenix cells.

Count PhxE cells from Murphy lab.

Count 5 squares = 50 cells

$5 \times 0.004 = 0.02\ mm^2$

$50 / 0.02 = 2500\ cells/mm^3 \times 10^3 = 2.5 \times 10^6\ cells/ml$

Seed $5 \times 10^6$ PhxE cells into a T75 flask (2 ml + 10 ml DMEM/FBS/PS).

10% FBS
1× sodium pyruvate
1× L-Glutamine
1× NEAA
1× P/S
1× β-ME (1 ml β-ME in 260 ml IMDM = 1000× stock filter-sterilized)

One flask per construct:

1. WT HVEM
2. P17A
3. Y23A
4. V36A

---

Mix 40 ml media + 40 µl chloroquine (1000× stock).

Add 10 ml per T75 flask immediately before transfection.
Measure DNA concentrations of plasmids
Mix:

| | **25 µg DNA** | **H2O (to 1095 µl)** |
|---|---|---|
| WT HVEM | 302.7 ul | 792.3 ul |
| P17A | 18.7 ul | 1076.3 ul |
| Y23A | 42.5 ul | 1052.5 ul |
| V36A | 53.9 ul | 1041.1 ul |

Add 155 µl CaCl2 slowly.
While bubbling, add 1250 µl 2×HBS (pH 7.05).
Mix and immediately add to the cells.

After 2 hrs, you should observe small black particles evenly distributed.
After 10-12 hrs, replace with 10 ml fresh media. → 37° O.N.

---

Replace with 10 ml fresh media, and move to 32° O.N.
Look for GFP expression.

Collect supernatant containing virus
(no need to spin it and concentrate it, since 293s are much easier to transfect.)
Replace media and return to 32° O.N.
Add virus supernatant to the HEK293 cells in the 6-well plate. Incubate at 37° O.N.

---

Collect supernatant containing virus again. Freeze some down at -80°.
Add more virus supernatant to the HEK293 cells in the 6-well plate. Incubate at 37° O.N.

---

Check for GFP expression.
Replace with fresh media.

---

Flow Data:

| **Cells** | **Treatment** | **% Total** | **% Difference** | **Events** |
|---|---|---|---|---|
| Non-transfected | none | 0.28 | | 55 |
| Non-transfected | tetramer | 0.45 | | 91 |
| Non-transfected | HVEM ab | 0.17 | | 34 |
| WT HVEM | none | 0.53 | 189.285714 | 106 |
| WT HVEM | tetramer | 1.47 | 326.666667 | 293 |
| WT HVEM | HVEM ab | 1.58 | 929.411765 | 316 |
| P17A | tetramer | 1.34 | 91.1564626 | 268 |
| P17A | HVEM ab | 1.8 | 87.7777778 | 360 |
| Y23A | tetramer | 0.54 | 36.7346939 | 108 |
| Y23A | HVEM ab | 0.54 | 34.1772152 | 107 |
| V36A | tetramer | 1.14 | 77.5510204 | 229 |
| V36A | HVEM ab | 1.01 | 63.9240506 | 203 |

I graphed both tetramer and HVEM to compare the ability to recognize the HVEM antibody versus the ability of HVEM to bind the tetramer.

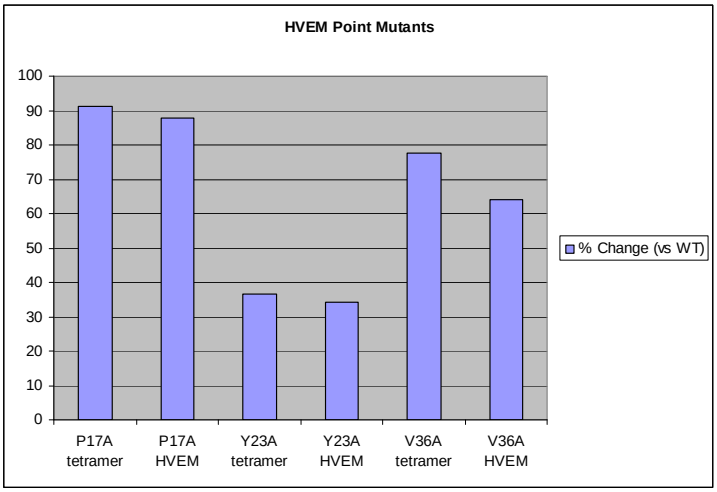


## HVEM-BTLA Flow Results

1) Non-transfected = 0.28% 55 events

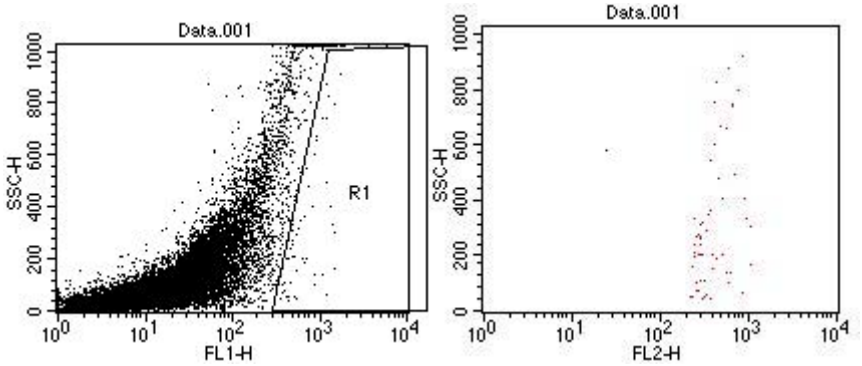


3) Non-transfected + Tetramer = 0.45% 91 events

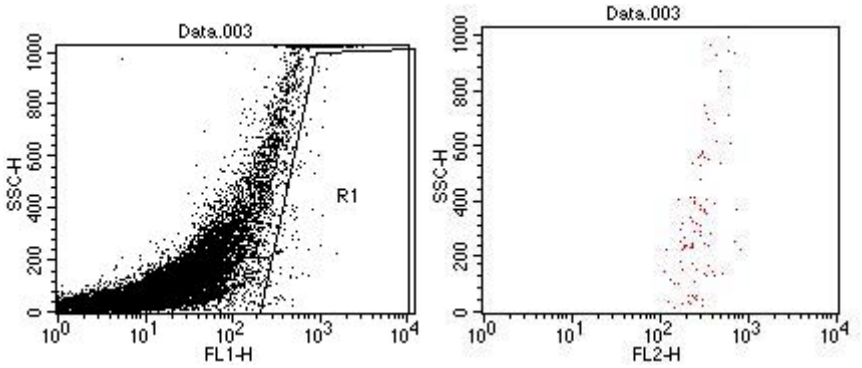


8) Non-transfected + HVEM = 0.17% 34 events

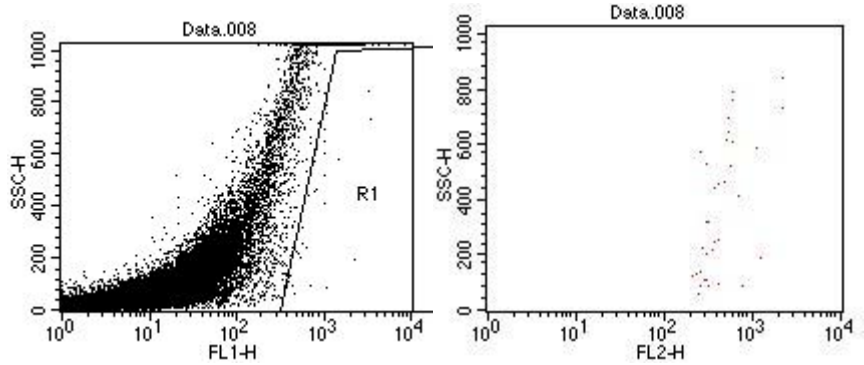


2) WT, No treatment = 0.53% 106 events

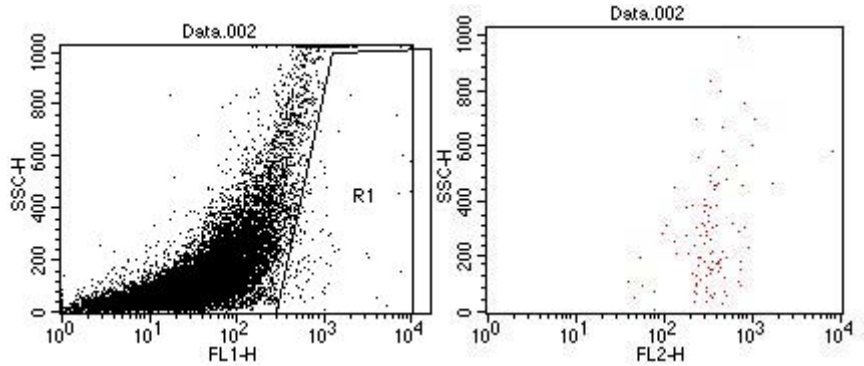


7) WT + Tetramer = 1.47% 293 events

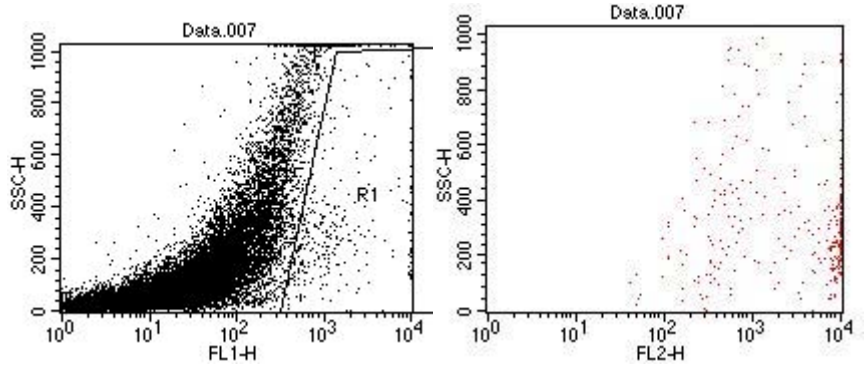


12) WT + HVEM = 1.58% 316 events

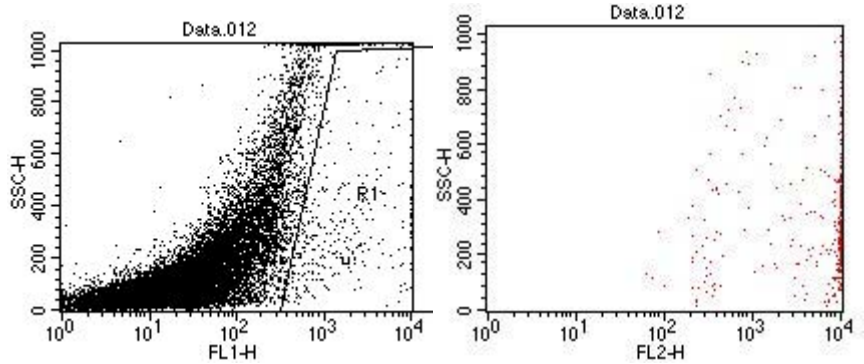


6) P17A + Tetramer = 1.34% 268 events

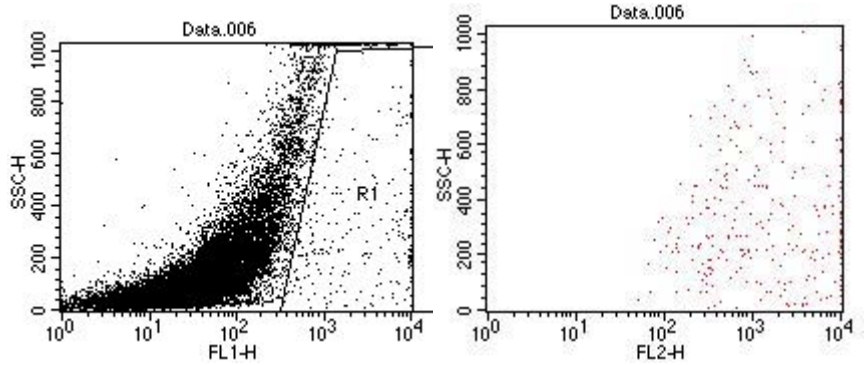


11) P17A + HVEM = 1.80% 360 events

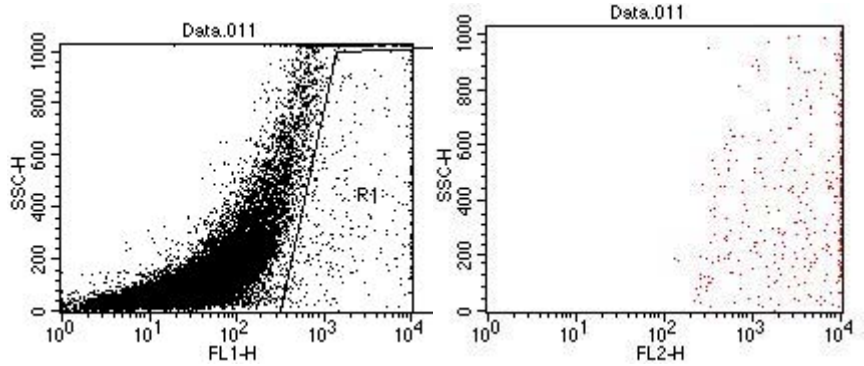


5) Y23A + Tetramer = 0.54% 108 events

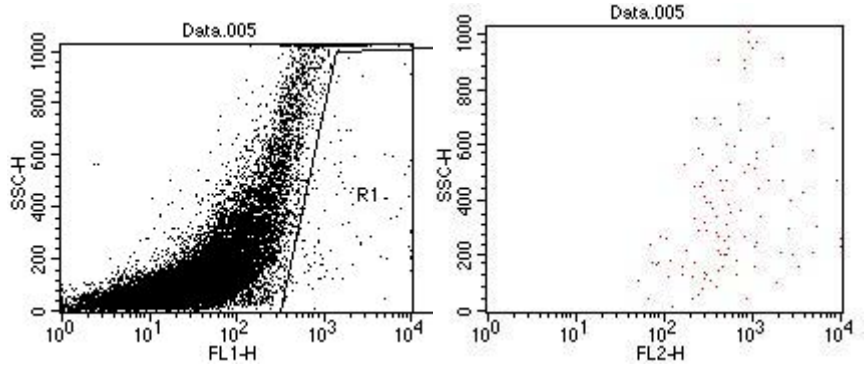


9) Y23A + HVEM = 0.54% 107 events

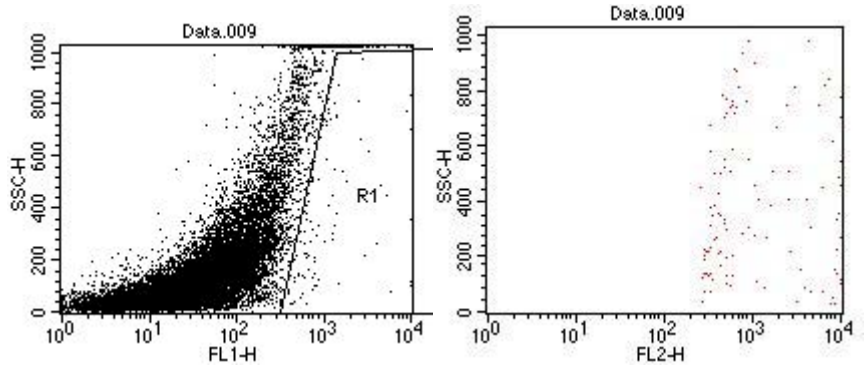


4) V36A + Tetramer = 1.14% 229 events

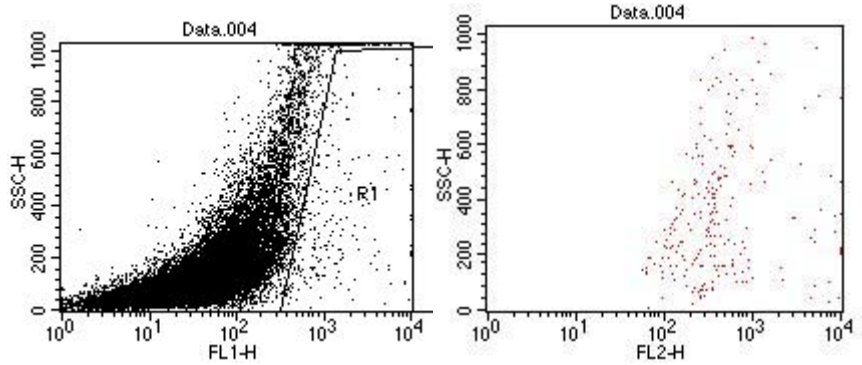


10) V36A + HVEM = 1.01% 203 events

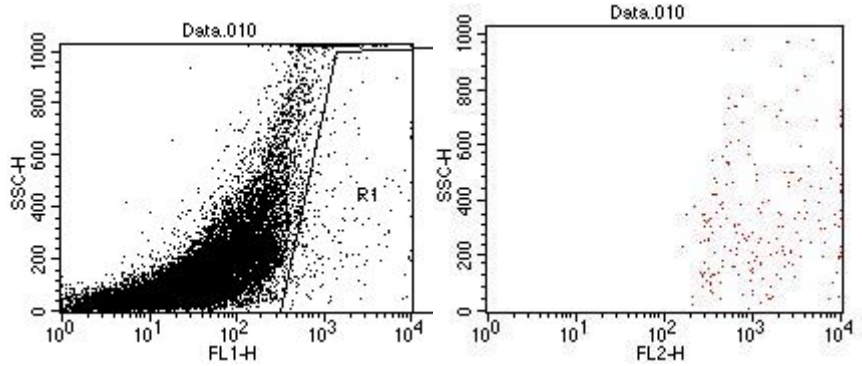


**Flow Data – Repeat Experiment**

| | No Antibody or Tetramer (Negative Control) | HVEM Antibody (Confirm expression) | BTLA Tetramer (Confirm BTLA binding) |
|---|---|---|---|
| Non-Transfected | 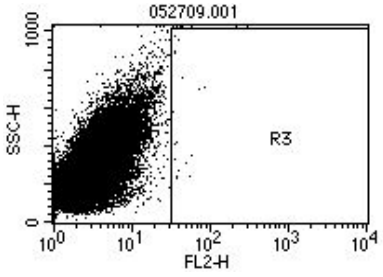  | 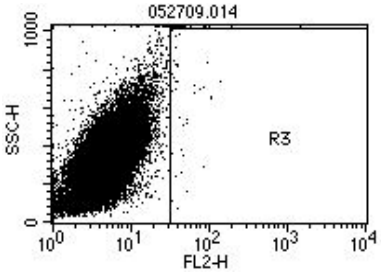  | 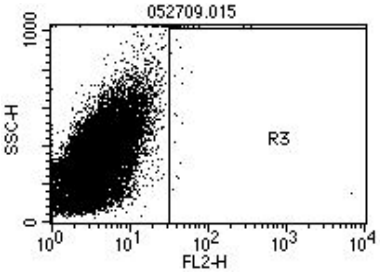  |
| WT HVEM | 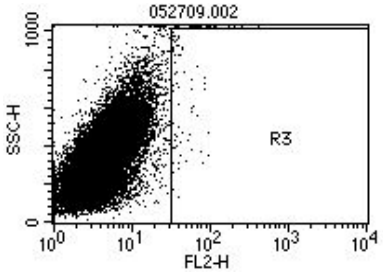  | 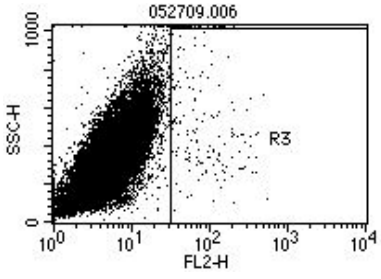  | 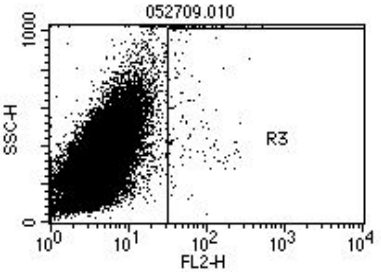  |

P17A Mutant

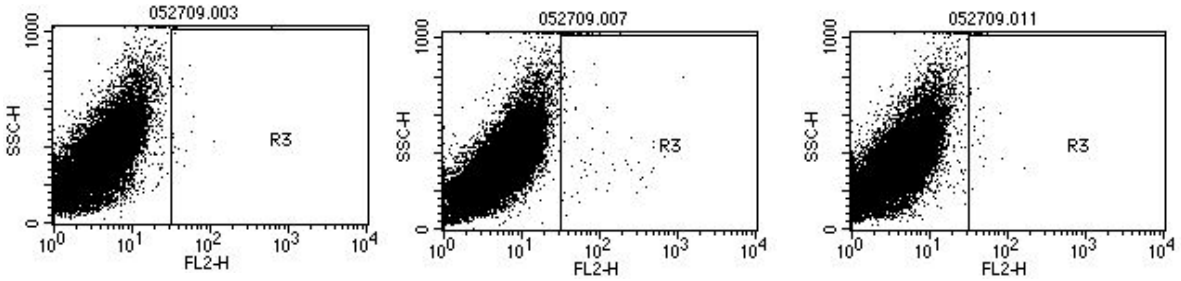


Y23A Mutant

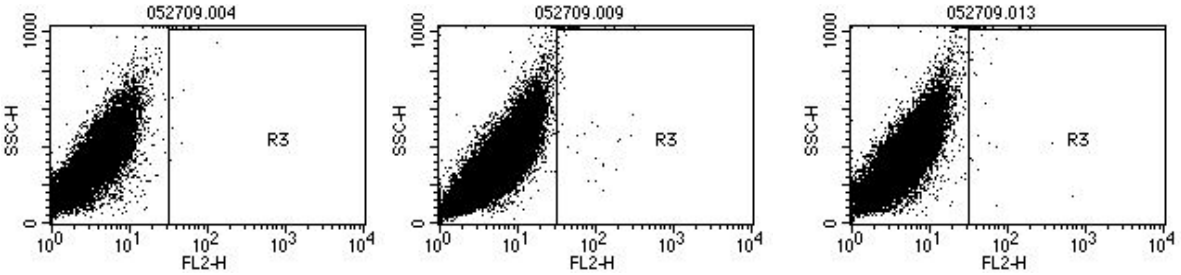


V36A Mutant

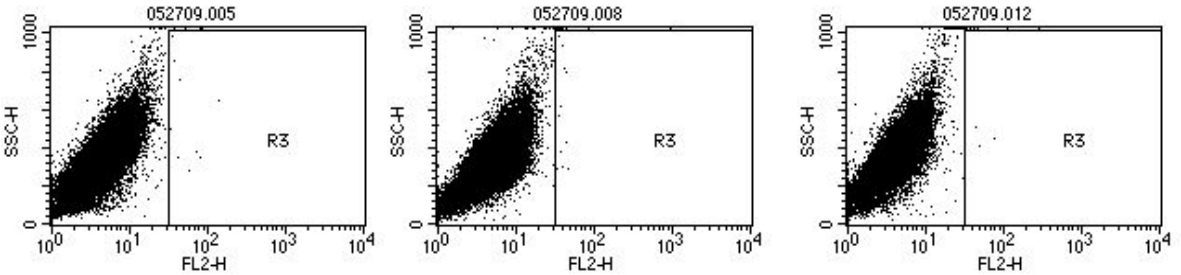


**Interpretation:** These studies demonstrate that the P17A, Y23A and V36A mutants were successfully created by site-directed mutagenesis. WT HVEM, P17A and Y23A appear to react with the HVEM mAb, although staining levels are low suggesting that the viral transduction needs to be optimized. WT HVEM, but not P17A or Y23A, reacts with BTLA tetramer, consistent with our hypothesis and structural data suggesting that these sites are critical for BTLA interaction. V36 A does not stain for HVEM mAb or BTLA tetramer suggesting that this viral transduction was not successful.

**Appendix #3: Manuscript submitted to *Nature Immunology***

# Anti-B and T lymphocyte attenuator treatment prevents Graft-versus-Host Disease and expands donor-derived regulatory T cells

Jörn C. Albring[1,2,*], Michelle M. Sandau[1,*], Stephanie K. Lathrop[3], Chyi-Song Hsieh[3], Matthias Stelljes[4], Theresa L. Murphy[1], and Kenneth M. Murphy[1,2]

[1]Department of Pathology and Immunology, Washington University School of Medicine, St. Louis, Missouri, USA. [2]Howard Hughes Medical Institute, Washington University School of Medicine, St. Louis, Missouri, USA. [3]Department of Medicine, Division of Rheumatology, Washington University School of Medicine, St. Louis, Missouri, USA. [4]Department of Medicine/Hematology and Oncology, University of Muenster, Muenster, Germany

*These authors contributed equally to this work.

Correspondence to: Kenneth M. Murphy, kmurphy@wustl.edu

**Abstract**

**Graft-versus-host disease (GVHD) causes significant morbidity in allogeneic stem cell transplantation (aHSCT), preventing its broader application to non-life threatening diseases. Here we show that a single administration of a non-depleting monoclonal antibody specific for B and T lymphocyte attenuator (BTLA)[1] permanently prevented GVHD when administered at the time of aHSCT. Once GVHD was established, anti-BTLA treatment was unable to reverse disease, suggesting its mechanism occurs early after aHSCT. Anti-BTLA treatment prevented GVHD independently of herpesvirus entry mediator (HVEM) and required BTLA expression by donor-derived T cells. Further, anti-BTLA treatment led to the expansion of pre-committed donor-derived regulatory T cells relative to effector T cells. These results suggest that BTLA agonism rebalances homeostatic T cell expansion in lymphopenic hosts following aHSCT, favoring Treg expansion at the expense of pathogenic effector T cells, thereby preventing GVHD. Thus, targeting BTLA at the initiation of aHSCT therapy might reduce limitations imposed by histocompatibility and allow broader application to treatment of non-life threatening diseases.**

Replacement of an abnormal or malignant lymphohematopoietic system by allogeneic haematopoietic stem-cell transplantation (aHSCT) from a healthy donor is an effective treatment for many disorders of the hematopoietic system[2-4]. Induction of a mixed hematopoietic donor-host chimerism can induce long-lasting tolerance to foreign tissues without the need for life-long immunosuppressive therapy[5-7]. aHSCT therapy has been improved by better donor identification[8], conditioning regimens that are more easily tolerated[9], and by enhanced supportive care[10]. However, significant treatment-related morbidity and mortality from chemotherapy, radiotherapy, infections and Graft-versus-Host Disease (GVHD) remain significant clinical problems. For these reasons, aHSCT is commonly indicated only for treatment of conditions where other treatments options are far inferior or lacking.

Costimulatory molecules of the CD28 family expressed by donor-derived T cells regulate GVHD, with inhibitory and activating receptors either decreasing or increasing its severity, respectively. Members of the TNF family of ligands and receptors also regulate GVHD[11-18]. BTLA is an inhibitory immunoglobulin superfamily receptor, whose ligand is the TNF receptor family member HVEM, and which has only been examined in a model of chronic allostimulation using non-irradiated hosts that do not develop GVHD[19]. The role of BTLA in aHSCT using irradiated recipients, in which clinical symptoms similar to human GVHD develop, has not been examined.

To determine the role of BTLA in the development of GVHD, we first examined wild type and $BTLA^{-/-}$ donor mice[20] using a parental-into-irradiated F1 model of allogeneic bone morrow transplantation (BMT)[21]. In this model, GVHD results from partial MHC mismatch between $H\text{-}2^{b}$ haplotype parental donor cells and lethally

irradiated H-2$^{b/d}$ haplotype recipients. Bone marrow and splenocytes from wild type or BTLA$^{-/-}$ mice were transferred into lethally irradiated CB6F1 recipients (**Fig. 1a**). Transplantation of wild type donor cells into CB6F1 recipients caused a decrease in body weight of approximately 30%, and generated clinical scores[22] of around 3 which persisted for greater than 40 days. BTLA$^{-/-}$ donor cells caused GVHD of similar magnitude as wild type donor cells, suggesting BTLA expressed by donor cells does not normally regulate disease in this model. To test whether BTLA expressed by recipient mice might also regulate GVHD in this model, we used lethally irradiated BTLA$^{-/-}$ CB6F1 hosts as recipients of BTLA$^{-/-}$ bone marrow and splenocytes (**Supplementary Fig. 1b**). BTLA$^{-/-}$ donor cells induced similar weight loss and GVHD clinical scores in BTLA$^{+/-}$ and BTLA$^{-/-}$ hosts, and similar disease caused by BTLA$^{+/+}$ donor cells (**Fig. 1a**). Collectively, these data suggest that in this model of GVHD, BTLA does not engage its ligand HVEM either on donor or recipient cells, and therefore can not act to regulate the development of GVHD.

However, since BTLA generates inhibitory signals[20,23,24] and functions in autoimmunity[20], malaria infection[25] and intestinal inflammation[26], we wondered whether harnessing the attenuating effects of BTLA on the immune response by forced engagement would have a regulatory effect on the development of GVHD. To test this possibility we compared the effects of an IgG1 hamster anti-BTLA monoclonal antibody[1,25], 6A6, administered at the time of BMT (**Fig. 1b**) with a control antibody, PIP, that recognizes bacterial GST[27]. Mice treated with PIP showed similar progression of GVHD as mice without antibody treatment (**Fig. 1a**), with clinical scores between 3 and 4 persisting for greater than 140 days (**Supplementary Fig. 1a**). These mice

developed GVHD associated with thickening of the lamina propria and muscularis, with severe inflammation and ulceration of the colon[21] (**Fig. 1c,** right panel). In contrast, a single treatment of 10 μg/g body weight of 6A6, given at the time of BMT, prevented GVHD completely (**Fig. 1b**), with no signs of clinical disease developing for the entire experimental period of 140 days after BMT (**Supplementary Fig. 1a**). Further, 6A6-treated mice had no evidence of GVHD in the colon, with lamina propria and muscularis showing no histological cellular infiltrates. Thus, a single administration of anti-BTLA antibody at the time of BMT prevents GVHD, eliminating weight loss, clinical signs of disease and histological changes in target organs.

We next asked if 6A6 acted by simply depleting donor T cells that express BTLA. CFSE-labeled donor cells were transferred into wild type recipients that were simultaneously treated either with control (PIP), 6A6, or with 6F7, a murine IgGκ anti-BTLA antibody known to cause *in vivo* depletion of BTLA-expressing cells[28]. Two days after transfer, we found similar numbers of $CFSE^+$ cells in mice that received either control or 6A6 antibody treatment (**Supplementary Fig. 2a**, upper panel), and no significant differences between numbers of $CD19^+$, $CD4^+$ or $CD8^+$ lymphocytes (lower panel). However, treatment with 6F7 caused a significant depletion of $CFSE^+$ lymphocytes, particularly from the $CD19^+$ cell population (**Supplementary Fig. 2a**). Furthermore, 6A6 was still detectable as bound to live donor-derived cells *in vivo* up to 7 days after transfer (**Supplementary Fig. 2b**). In addition, 6A6 treatment was unable to prevent GVHD caused when $BTLA^{-/-}$ donors were used as a source of bone marrow for BMT **(Supplementary Fig. 2c**). Thus, 6A6 does not act by *in vivo* depletion of donor-derived lymphocytes, but requires the expression of BTLA on donor cells.

To determine how 6A6 prevented GVHD, we asked if 6A6 could reverse established GVHD if administered at later times after BMT. We compared immediate administration of 6A6 with delayed administration given 14 days after BMT (**Fig. 2a**). Again, 6A6 administration concurrent with BMT prevented GVHD. In contrast, there was no statistical difference in weight loss or clinical scores between mice that received 6A6 14 days after BMT compared to mice that received PIP control antibody (**Fig. 2a**).

6A6 binds to a region of BTLA that is involved in interactions with HVEM[1,29]. Thus, 6A6 might prevent GVHD by preventing interactions between HVEM on donor cells with BTLA on recipient cells, blocking co-stimulatory signaling to donor cells[14]. Even though our data already indicated that host BTLA is not involved (**Supplementary Fig. 1c**), we wished to test this possibility independently. Thus, we asked whether 6A6 could prevent GVHD after BMT using $HVEM^{-/-}$ donor cells **(Fig. 2b**). Transfer of $HVEM^{-/-}$ donor cells caused induction of GVHD when administered with control antibody (**Fig. 2b**). The severity of GVHD caused by $HVEM^{-/-}$ donor cells was somewhat less than that caused by wild type donor cells (**Fig. 1b**), consistent with a report that HVEM and LIGHT are co-stimulatory in promoting GVHD[14]. However, 6A6 also prevented the GVHD caused by $HVEM^{-/-}$ donor cells (**Fig 2b**), both preventing weight loss and completely eliminating disease scores. These results indicate that 6A6 prevents GVHD in a manner that is independent of HVEM, suggesting it acts directly through BTLA expressed by donor cells.

Although the precise molecular targets of BTLA signaling are still obscure[23,30,31], BTLA engagement by HVEM can inhibit T cell proliferation *in vitro* [32] and promote tolerance induction *in vivo*[33]. Therefore we asked if 6A6 treatment alters donor T cell

proliferation or IL-2 production *in vivo*. CFSE-labeled donor splenocytes were transferred into lethally irradiated CB6F1 recipients that were treated with either control antibody or 6A6, and donor T cell proliferation was assessed after 3 and 7 days. Proliferation $CD4^+$ and $CD8^+$ T cells measured by CFSE dilution was similar in recipient mice treated with control or 6A6 antibody (**Supplementary Fig. 3c**). However, 6A6 treatment significantly reduced the total accumulation of donor $CD4^+$ and $CD8^+$ T cells compared to control. Accumulation of donor-derived $CD4^+$ T cells in 6A6-treated mice was approximately 70% less than in PIP-treated mice on day 3, and 50% less than PIP-treated mice on day 7 after BMT (**Supplementary Fig. 3a, b**). In addition, the accumulation of donor-derived $CD8^+$ T cells was reduced in 6A6-treated mice relative to PIP-treated mice, although not as dramatically as for $CD4^+$ T cells. However, IL-2 production 7 days after BMT was not statistically different between $CD4^+$ T cells in 6A6-treated and PIP-treated mice (**Supplementary Fig. 4**). A small but statistically significant reduction in interferon (IFN)-γ production was observed in $CD4^+$ T cells from 6A6-treated mice compared to controls, but no differences in IL-17 and IL-4 production (**Supplemental Fig. 4**). In summary, 6A6 administered at the time of BMT reduced accumulation of donor-derived effector T cells without inducing anergy, inhibiting IL-2 production or causing major alterations in cytokines.

These effects were suggestive of the actions of regulatory T cells (Tregs) expressing the transcription factor forkhead box P3 (Foxp3)[34]. Tregs have recently been reported to play a significant role in regulating GVHD[35-38], and there are ongoing clinical trials aimed directly at the use of Treg cells as an intervention in human GVHD (NCI clinical trial NCT00725062).

Thus, to determine whether 6A6 treatment influences Tregs, we measured endogenous Foxp3 expression in donor-derived $CD4^+$ T cells 7 days after BMT (**Fig. 3a**). We first examined transfer of WT donor cells in CB6F1 recipients. In PIP-treated recipients, which developed GVHD, 11 ± 0.7 % ($n$ = 5) of donor-derived $CD4^+$ T were found to express Foxp3 (**Fig. 3b**), whereas in 6A6-treated mice, which did not develop GVHD, 41 ± 1.8 % ($n$ = 5) of donor-derived $CD4^+$ T cells expressed Foxp3 (**Fig. 3b**). Thus, 6A6 treatment increases the numbers of donor-derived Tregs after BMT. Since BTLA is expressed by several hematopoietic cell types[1], 6A6 treatment could increase Tregs either by direct engagement on $CD4^+$ donor T cells or by indirect engagement of BTLA expressed by host antigen presenting cells (APCs). To distinguish these possibilities, we performed mixed BMT using WT (CD45.1) and $BTLA^{-/-}$ (CD45.2) mice as donors for BMT. If 6A6 treatment increases Foxp3 expression directly, then $BTLA^{-/-}$ T cells should be unaffected by 6A6, whereas indirect actions through host APCs should affect WT and $BTLA^{-/-}$ donor cells. We found that 6A6 treatment selectively increased Foxp3 expression only in WT, but not in $BTLA^{-/-}$, donor T cells (**Fig. 3a, c**). In PIP-treated (control) recipients, 14 ± 2.4 % ($n$ = 5) of donor-derived WT (CD45.1) $CD4^+$ T expressed Foxp3 (**Fig. 3c**), whereas in 6A6-treated mice, 48 ± 4.5 % ($n$ = 5) donor-derived WT $CD4^+$ T cells expressed Foxp3 (**Fig. b**). However, 6A6 failed to increase Foxp3 expression in $BTLA^{-/-}$ (CD45.2) donor-derived $CD4^+$ T cells (7.8 ± 0.9 %; $n$ = 5) compared to PIP-treated controls (7.3 ± 0.9 %; $n$ = 5). These results suggest that 6A6 treatment increases Treg frequency after BMT through direct engagement of BTLA expressed by donor-derived $CD4^+$ T cells.

6A6 treatment could increase Treg frequency either by inducing Foxp3 expression in naïve donor $CD4^+$ T cells[39] or by causing *in vivo* expansion of pre-existing donor $Foxp3^+$ T cells relative to $Foxp3^-$ T cells. To distinguish these alternatives, we used *B6.Foxp3$^{gfp}$* mice[40], in which endogenous Foxp3 has been replaced by a chimeric GFP-Foxp3 fusion protein. We performed mixed BMT with WT (CD45.1) and *Foxp3$^{gfp}$* (CD45.2) mice as donors for BMT, using purified GFP-negative cells from *Foxp3$^{gfp}$* mice to remove pre-existing Tregs from the CD45.2 donor population. In this mixed BMT setting, 6A6 treatment increased the frequency of $Foxp3^+$ donor-derived T cells only in the WT (CD45.1) donor T cells, but not in the *Foxp3$^{gfp}$* (CD45.2) donor T cells as assessed by intracellular staining for endogenous Foxp3 (**Fig. 4a, b**). In addition, these donor-derived $CD4^+$ T cells, that were originally isolated from *B6.Foxp3$^{gfp}$* mice as negative for GFP expression, remained negative for Foxp3 as assessed by the GFP-Foxp3 fusion protein reporter (**Fig. 4c**). As a control, we administered 6A6 to unmanipulated *B6.Foxp3$^{gfp}$* mice, and examined the frequency of $Foxp3^+$ $CD4^+$ cells after 6 days (**Supplementary Fig. 5**). In this case, there was no change in the frequency of Foxp3 expression in $CD4^+$ T cells, suggesting that the effect of 6A6 treatment requires the context of T cell activation and homeostatic proliferation *in vivo.*

In summary, this study demonstrates that 6A6 administered once at the time of allogeneic BMT permanently prevents GVHD through a unique mechanism of action, involving the direct engagement of donor-derived T cells and leading to the relative expansion of pre-existing $CD4^+$ Tregs compared to pathogenic effector cells. Established GVHD was not reversed by 6A6 treatment, suggesting early expansion of Tregs is critical for achieving a suppressive environment of alloreactive donor T cells. Thus, BTLA may

represent a novel therapeutic target in treatment of aHSCT. Eliminating the risks of aHSCT, such as GVHD and the requirement for chronic immunosuppressive, could potentially allow its application more widely as a tolerogenic therapy in treatment of autoimmune disorders or solid organ transplantation, for which it is currently performed only experimentally[4-7].

## Material and Methods

**Mice and bone marrow transplantation** B6.SJL-Ptprca Pep3b/BoyJ (B6.SJL), C57BL/6, and C57BL/6 x BALB/c F1 (CB6F1) mice were obtained from The Jackson Laboratory (Bar Harbor, ME) or bred in our facility. *BTLA*$^{-/-}$[20], *Hvem*$^{-/-}$[41], and *Foxp3*$^{gfp}$[40] mice were backcrossed to C57BL/6 for at least nine generations. Mice were 12–18 weeks old and female. All mice were kept under special pathogen-free conditions.

**Cell transplantation and assessment of GVHD** Mice received transplants according to a standard protocol as previously described[21]. Briefly, bone marrow cells were harvested by flushing tibia and femurs of donor mice. For GVHD induction, CB6F1 (H-2$^{b/d}$) recipients were lethally irradiated with 9 Gy total body irradiation (TBI) using a $^{137}$Cs source at a dose rate of ~70 cGy/minute and reconstituted with bone marrow cells (BMCs) and additional splenocytes ($2x10^7$ BMCs and $1x10^7$ splenocytes) from indicated donors (H-2$^{d}$). GVHD was monitored by calculating the loss in total body weight. Body weights were measured before transplantation and 3 times a week after transplantation.

Clinical GVHD intensity was scored by assessing weight loss, posture, activity, fur texture, and skin integrity[22]. Histopathologic analyses of the bowel were performed on hematoxylin and eosin (H&E)–stained tissue. Microscopic analyses were performed with a BX51 light microscope (Olympus, Hamburg, Germany) equipped with a 40x/0.75 NA objective lens and a DP70 camera (Olympus) using Cell A Analysis software (Olympus Software Imaging Solutions 1986-2007, Muenster, Germany). Experiments were performed in accordance with national and institutional guidelines.

**Administration of antibody** In some experiments mice received a single intraperitoneal injection of 10-20 μg/g body weight of the IgG1 hamster monoclonal anti-BTLA antibody 6A6, the IgGκ mouse monoclonal anti-BTLA antibody 6F7 (ref [1]) or the hamster monoclonal anti-GST antibody PIP[27] at indicated time points.

**CFSE labeling and Flow Cytometery** Cells were labeled with CFSE (carboxyfluorescein diacetate succinimidyl diester; Sigma-Aldrich) by being incubated for 8 min at 25 °C with 1μM CFSE at a density of $40 \times 10^6$ cells per ml in PBS. Labeling was quenched by incubation of cells for 1 min with an equal volume of FCS and cells were washed twice with media containing 10% (vol/vol) FCS. $50 \times 10^6$ total cells per mouse were injected intravenously. Single cell suspensions from spleens were analyzed by flow cytometry using the following antibodies for detection: $K^d$-FITC (SF1-1.1), CD4-PECy7 and APC (RM4-5), anti–Armenian and Syrian hamster IgG cocktail-PE, CD19-APC (1D3) purchased from BD Pharmingen. Additional antibodies purchased from eBioscience were also used: CD45.1-PECy7 and APC (A20), CD8-APC AlexaFluor 750 (53-6.7), CD4-APC AlexaFluor 750 (RM4-5). Intracellular Foxp3 was detected using eBioscience Mouse Regulatory T cell staining Kit with Foxp3-PE or APC (FJK-

16s). For intracellular cytokine staining splenocytes were first restimulated with PMA/ionomycin for 4 hours and were stained with antibodies to surface markers followed by fixation with 2% formaldehyde for 15 minutes at room temperature. Cells were then washed once in 0.05% saponin and stained with anti-cytokine antibodies (anti-IL-17 FITC, IL-2 PE, IFNγ PE-Cy7 and IL-4 APC) in 0.5% saponin. All flow cytometry data were collected on a FACSCanto II (BD Biosciences) and were analyzed with FlowJo software (Tree Star).

**Statistical analysis** A Student's unpaired two-tailed t-test with a 95% confidence interval was used for statistical analyses of body weight data and cell numbers. Differences with P values of 0.05 or less are considered significant.

**Figure Legends**

**Figure 1** Anti-BTLA treatment permanently prevents graft-vs-host disease. (**a**) CB6F1 mice were lethally irradiated and received 2.0 x $10^7$ BMCs and 1.0 x $10^7$ splenocytes from parental C57BL/6 $BTLA^{+/+}$ (closed squares) or $BTLA^{-/-}$ (open squares) donors. (**b**) CB6F1 were lethally irradiated and received 2.0 x $10^7$ BMCs and 1.0 x $10^7$ splenocytes from parental C57BL/6 $BTLA^{+/+}$ mice and a single 200 μg injection intraperitoneally of the control antibody PIP (open circles) or the antibody 6A6 (closed circles). (**c**) Histopathology of the colon 143 days after BMT of animals that had received a single injection of 6A6 (left panel) or the control antibody PIP (right panel) on the day of BMT. Original magnification for histopathology was 4x. Body weight loss and a clinical score were used as a measure of GVHD in recipient mice after BMT. Error bars indicate positive standard deviations for each time point. *Statistically significant differences versus both control groups ($P < .05$).

**Figure 2** Anti-BTLA treatment exerts its affects at the time of BMT and does not block BTLA-HVEM interactions. (**a**) CB6F1 mice were lethally irradiated and received 2.0 x $10^7$ BMCs and 1.0 x $10^7$ splenocytes from parental C57BL/6 $BTLA^{+/+}$ mice together with either a single 200 μg injection intraperitoneally of control antibody (open circles) or 6A6 (closed circles) on the day of BMT or a single 200 μg injection of 6A6 14 days after BMT (triangles). Body weight loss and a clinical score were used as a measure of GVHD in recipient mice after BMT. (**b**) CB6F1 were lethally irradiated and received 2.0 x $10^7$ BMCs and 1.0 x $10^7$ splenocytes from parental C57BL/6 $HVEM^{-/-}$ mice and a single 200 μg injection intraperitoneally of control antibody PIP (open circles) or 6A6

(closed circles). Body weight loss and a clinical score were used as a measure of GVHD in recipient mice after BMT. Error bars indicate positive standard deviations for each time point. *Statistically significant differences versus both control groups ($P < .05$).

**Figure 3** Direct engagement of BTLA on donor CD4 T cells leads to an increased frequency of $CD4^+$ $Foxp3^+$ cells. CB6F1 ($CD45.1^-H\text{-}2K^{d+}$) mice were lethally irradiated and received either 2.0 x $10^7$ BMCs and 1.0 x $10^7$ B6.SJL $BTLA^{+/+}$ splenocytes alone (**b**) or a 1:1 mixture of B6.SJL $BTLA^{+/+}$ ($CD45.1^+H\text{-}2K^{d-}$) and C57BL/6 $BTLA^{-/-}$ ($CD45.1^-H\text{-}2K^{d-}$) donor cells (**a** and **c**) with either a single 200 µg injection intraperitoneally of control antibody or 6A6. After 7 days splenocytes were stained for CD45.1, $H\text{-}2K^d$, CD4, and intracellularly for FoxP3. a) Shown are plots for CD45.1 and $H\text{-}2K^d$ (left) and CD4 and FoxP3 (right) gated on C57BL/6 $BTLA^{-/-}$ ($CD4^+CD45.1^-$ $H\text{-}2K^{d-}$) or C57BL/6 $BTLA^{+/+}$ ($CD4^+CD45.1^+$ $H\text{-}2K^{d-}$) donor cell populations as indicated. Numbers represent the percentage of cells within the indicated gates. (**b**) Shown are the percentage of $CD45.1^+CD4^+Foxp3^+$ cells as a percentage of all $CD45.1^+CD4^+$ B6.SJL $BTLA^{+/+}$ derived donor cells. Data shown are mean ± SEM (n = 5). (**c**) Same experiment as in a). Shown are the percentage of $CD4^+Foxp3^+$ cells as a percentage of all donor $CD4^+$ cells from either B6.SJL $BTLA^{+/+}$ mice (left) or from C57BL/6 $BTLA^{-/-}$ mice (right) that received either control antibody (open bars) or 6A6 (filled bars). Data shown are mean ± SEM (n = 5)

**Figure 4** Anti-BTLA treatment allows relative expansion of pre-exisiting donor-derived Tregs after BMT. CB6F1 ($CD45.2^+$ $H\text{-}2K^{d+}$) mice were lethally irradiated and received

2.0 x $10^7$ BMCs and 1.0 x $10^7$ WT B6.SJL ($CD45.1^+$ $H\text{-}2K^{d-}$) splenocytes along with 1x$10^6$ purified $CD4^+$ Foxp3-negative T cells from *B6.Foxp3$^{gfp}$* mice ($CD45.2^+$ $H\text{-}2K^{d-}$) with either a single intraperitoneal 200 μg injection of control antibody or 6A6. After 7 days, splenocytes were stained for CD45.1, CD45.2, $H\text{-}2K^d$, CD4, and intracellular expression of Foxp3. Foxp3 expression was also determined by GFP expression. (**a**) Donor cells are identified by the lack of $H2\text{-}K^d$ and the expression of CD4, and CD45.2 or CD45.1 is used to determine the origin of the donor. Expression of intracellular Foxp3 within $CD4^+$ T cells from the WT donor ($CD5.1^+$) is shown. (**b**) Shown are the percentage of $CD4^+FoxP3^+$ cells in (**a**) as a percentage of all donor $CD4^+$ cells from either WT donors (left) or from *B6.Foxp3$^{gfp}$* donors (right) that received either control antibody (open bars) or 6A6 (filled bars). Data shown are mean ± SEM (*n* = 5). (**c**) Expression of Foxp3 as reported by GFP from the *B6.Foxp3$^{gfp}$* donor ($CD45.2^+$) is shown.

**Supplementary Figure Legends**

**Supplementary Figure 1** BTLA expression by recipient tissue does not promote GVHD, but anti-BTLA treatment prevents GVHD long term. (**a**) Same experiment as in Figure 1b followed-up for 143 days. Body weight loss and a clinical score were used as a measure of GVHD in recipient mice after BMT. Error bars indicate positive standard deviations for each time point. (**b**) CB6F1 BTLA$^{+/-}$ mice (closed squares) or CB6F1 BTLA$^{-/-}$ (open squares) were lethally irradiated and received 2.0 x $10^7$ BMCs and 1.0 x $10^7$ splenocytes from parental C57BL/6 BTLA$^{-/-}$ donors. Body weight loss and a clinical score were used as a measure of GVHD in recipient mice after BMT. Data shown are mean ± SEM ($n$ = 5)

**Supplementary Figure 2** Treatment with anti-BTLA antibody 6A6 does not deplete lymphocytes. C57BL/6 mice received 5.0 x $10^6$ CFSE-labeled splenocytes from B6.SJL mice together with a single intraperitoneal injection of 200 μg of either control antibody PIP or anti-BTLA antibodies 6A6 or 6F7. After 2 days splenocytes were stained for CD4, CD8α, CD19, and anti-hamster (for 6A6 and PIP). (**a**) Shown are numbers of either all donor CFSE$^+$ cells (upper figure) or CD19$^+$, CD8$^+$, and CD4$^+$ subsets of CFSE$^+$ cells (lower figure) recovered from mice that had received either control antibody (open bars), 6A6 (filled bars) or 6F7 (shaded bars). Data shown are mean ± SEM ($n$ = 3). (**b**) CB6F1 (CD45.1$^-$) mice were lethally irradiated and received 5.0 x $10^7$ splenocytes from B6.SJL (CD45.1$^+$) mice together with a single intraperitoneal injection of 200 μg of either 6A6 or PIP. After 7 days splenocytes were stained for CD45.1 and anti-hamster. Shown is a histogram detecting bound antibody to lymphocytes read out by anti-hamster

intensity within the $45.1^+$ donor cell population of mice that had either received 6A6 (bold line) or PIP (shaded fill). (**c**) BMT were performed as described in **Fig. 1b**, except that $BTLA^{-/-}$ mice were used as donors.

**Supplementary Figure 3** CD4 T cell accumulation is modestly affected by 6A6 treatment while CD4 and CD8 T cell proliferation is unperturbed. CB6F1 ($CD45.1^-$) mice were lethally irradiated and received 5.0 x $10^7$ CFSE-labeled splenocytes from B6.SJL ($CD45.1^+$) mice together with a single intraperitoneal 200 μg injection of either the antibody 6A6 or the control antibody PIP. After 3 (**a**) and 7 (**b**) days splenocytes were stained for CD45.1, CD4, and CD8α. Shown are numbers of $CD4^+$ (left) or $CD8^+$ (right) cells of the $45.1^+$ donor cell population recovered from mice that had received either 6A6 (open bars) or PIP (filled bars). Data shown are mean ± SEM (*n* = 3). (**c**) Histograms of cell division history indicated by CFSE-intensity for $CD4^+$ (left) or $CD8^+$ (right) cells within the $45.1^+$ donor cell population on days 3 (upper panel) and 7 (lower panel) of mice that had either received 6A6 (bold line) or PIP (shaded fill).

**Supplementary Figure 4** 6A6 treatment does not alter cytokine production of donor CD4 T cells. CB6F1 ($CD45.1^-H\text{-}2K^{d+}$) mice were lethally irradiated and received 2.0 x $10^7$ BMCs and 1.0 x $10^7$ splenocytes from B6.SJL mice, and either control antibody or 6A6. 7 days after BMT splenocytes were harvested and stimulated with PMA/Ionomycin for 5 hours. Following restimulation, cells were stained for CD4, and either IL-2, IFN-γ, IL-17 and IL-4 or Isotype controls for the cytokines. (**a**) Plots show $CD4^+$ cells and FSC, then gated on all $CD4^+$ cells Isotype controls for control and 6A6

treated mice top 2 rows. Bottom two rows show the production of the indicated cytokine following either control or 6A6 treatment. (**b**) The percentage of $CD4^+$ cells shown in (**a**) producing the indicated cytokine are shown as mean ± SEM ($n$ = 3).

**Supplementary Figure 5** 6A6 does not expand steady state Tregs. *B6.Foxp3$^{gfp}$* mice were given an intraperitoneal injection of 200 μg of either control antibody PIP or 6A6 and splenocytes were harvested 6 days later. Cells were stained with CD4, and expression of the GFP reporter was assessed. (**a**) Plots showing the percentage of all cells that express CD4 and Foxp3 following control antibody (left) or 6A6 treatment (right). (**b**) Same experiment as in (**a**) showing the percent of $FoxP3^+$ cells within $CD4^+$ T cells.

Reference List

1. Hurchla, M. A. et al., B and T lymphocyte attenuator exhibits structural and expression polymorphisms and is highly induced in anergic CD4(+) T cells. *Journal of Immunology* **174**, 3377-3385 (2005).

2. Appelbaum, F. R. The current status of hematopoietic cell transplantation. *Annu.Rev Med.* **54**, 491-512 (2003).

3. Copelan, E. A. Medical progress: Hematopoietic stem-cell transplantation. *New England Journal of Medicine* **354**, 1813-1826 (2006).

4. Sykes, M. and Nikolic, B. Treatment of severe autoimmune disease by stem-cell transplantation. *Nature* **435**, 620-627 (2005).

5. Alexander, S. I. et al., Brief report: Chimerism and tolerance in a recipient of a deceased-donor liver transplant. *New England Journal of Medicine* **358**, 369-374 (2008).

6. Kawai, T. et al., Brief report: HLA-mismatched renal transplantation without maintenance immunosuppression. *New England Journal of Medicine* **358**, 353-361 (2008).

7. Scandling, J. D. et al., Brief report: Tolerance and chimerism after renal and hematopoietic-cell transplantation. *New England Journal of Medicine* **358**, 362-368 (2008).

8. Petersdorf, E. W. et al., Limits of HLA mismatching in unrelated hematopoietic cell transplantation. *Blood* **104**, 2976-2980 (2004).

9. McSweeney, P. A. et al., Hematopoietic cell transplantation in older patients with hematologic malignancies: replacing high-dose cytotoxic therapy with graft-versus-tumor effects. *Blood* **97**, 3390-3400 (2001).

10. Gratwohl, A. et al., Cause of death after allogeneic haematopoietic stem cell transplantation (HSCT) in early leukaemias: an EBMT analysis of lethal infectious complications and changes over calendar time. *Bone Marrow Transplantation* **36**, 757-769 (2005).

11. Tamada, K. et al., LIGHT, a TNF-like molecule, costimulates T cell proliferation and is required for dendritic cell-mediated allogeneic T cell response. *J Immunol.* **164**, 4105-4110 (2000).

12. Tamada, K. et al., Modulation of T-cell-mediated immunity in tumor and graft-versus-host disease models through the LIGHT co-stimulatory pathway. *Nat.Med.* **6**, 283-289 (2000).

13. Tamada, K. et al., Blockade of LIGHT/LT beta and CD40 signaling induces allospecific T cell anergy, preventing graft-versus-host disease. *Journal of Clinical Investigation* **109**, 549-557 (2002).

14. Xu, Y. et al., Selective targeting of the LIGHT-HVEM co-stimulatory system for the treatment of graft-versus-host disease. *Blood*(2006).

15. Tsukada, N. et al., Blockade of CD134 (OX40)-CD134L interaction ameliorates lethal acute graft-versus-host disease in a murine model of allogeneic bone marrow transplantation. *Blood* **95**, 2434-2439 (2000).

16. Blazar, B. R. et al., Ligation of OX40 (CD134) regulates graft-versus-host disease (GVHD) and graft rejection in allogeneic bone marrow transplant recipients. *Blood* **101**, 3741-3748 (2003).

17. Blazar, B. R. et al., CD30/CD30 ligand (CD153) interaction regulates CD4(+) T cell-mediated graft-versus-host disease. *Journal of Immunology* **173**, 2933-2941 (2004).

18. Blazar, B. R. et al., Blockade of programmed death-1 engagement accelerates graft-versus-host disease lethality by an IFN-gamma-dependent mechanism. *Journal of Immunology* **171**, 1272-1277 (2003).

19. Hurchla, M. A., Sedy, J. R., and Murphy, K. M. Unexpected role of B and T lymphocyte attenuator in sustaining cell survival during chronic allostimulation. *The Journal of Immunology* **178**, 6073-6082 (2007).

20. Watanabe, N. et al., BTLA is a lymphocyte inhibitory receptor with similarities to CTLA-4 and PD-1. *Nat.Immunol.* **4**, 670-679 (2003).

21. Stelljes, M. et al., Clinical molecular imaging in intestinal graft-versus-host disease: mapping of disease activity, prediction, and monitoring of treatment efficiency by positron emission tomography. *Blood* **111**, 2909-2918 (2008).

22. Cooke, K. R. et al., An experimental model of idiopathic pneumonia syndrome after bone marrow transplantation .1. The roles of minor H antigens and endotoxin. *Blood* **88**, 3230-3239 (1996).

23. Gavrieli, M. et al., Characterization of phosphotyrosine binding motifs in the cytoplasmic domain of B and T lymphocyte attenuator required for association with protein tyrosine phosphatases SHP-1 and SHP-2. *Biochem Biophys.Res Commun.* **312**, 1236-1243 (2003).

24. Chemnitz, J. M. et al., B and T lymphocyte attenuator-mediated signal transduction provides a potent inhibitory signal to primary human CD4 T cells that can be initiated by multiple phosphotyrosine motifs. *The Journal of Immunology* **176**, 6603-6614 (2006).

25. Lepenies, B. et al., Ligation of B and T lymphocyte attenuator prevents the genesis of experimental cerebral malaria. *The Journal of Immunology* **179**, 4093-4100 (2007).

26. Steinberg, M. W. et al., A crucial role for HVEM and BTLA in preventing intestinal inflammation. *J Exp.Med.* **205**, 1463-1476 (2008).

27. Gronowski, A. M. et al., Baculovirus stimulates antiviral effects in mammalian cells. *Journal of Virology* **73**, 9944-9951 (1999).

28. Truong, W. et al., Combined Coinhibitory and Costimulatory Modulation with Anti-BTLA and CTLA4Ig Facilitates Tolerance in Murine Islet Allografts. *Am J Transplant* **7**, 2663-2674 (2007).

29. Nelson, C. A. et al., Structural determinants of herpesvirus entry mediator recognition by murine B and T lymphocyte attenuator. *The Journal of Immunology* **180**, 940-947 (2008).

30. Wu, T. H. et al., B and T lymphocyte attenuator interacts with CD3zeta and inhibits tyrosine phosphorylation of TCRzeta complex during T-cell activation. *Immunol Cell Biol*(2007).

31. Gavrieli, M. and Murphy, K. M. Association of Grb-2 and PI3K p85 with phosphotyrosile peptides derived from BTLA. *Biochem Biophys.Res Commun.* **345**, 1440-1445 (2006).

32. Sedy, J. R. et al., B and T lymphocyte attenuator regulates T cell activation through interaction with herpesvirus entry mediator. *Nat.Immunol.* **6**, 90-98 (2005).

33. Liu, X. K. et al., Cutting Edge: A Critical Role of B and T Lymphocyte Attenuator in Peripheral T Cell Tolerance Induction. *Journal of Immunology* **182**, 4516-4520 (2009).

34. Hori, S., Nomura, T., and Sakaguchi, S. Control of regulatory T cell development by the transcription factor Foxp3. *Science* **299**, 1057-1061 (2003).

35. Taylor, P. A., Lees, C. J., and Blazar, B. R. The infusion of ex vivo activated and expanded CD4(+)CD25(+) immune regulatory cells inhibits graft-versus-host disease lethality. *Blood* **99**, 3493-3499 (2002).

36. Cohen, J. L. et al., CD4(+)CD25(+) immunoregulatory T cells: New therapeutics for graft-versus-host disease. *Journal of Experimental Medicine* **196**, 401-406 (2002).

37. Hoffmann, P. et al., Donor-type CD4(+)CD25(+) regulatory T cells suppress lethal acute graft-versus-host disease after allogeneic bone marrow transplantation. *Journal of Experimental Medicine* **196**, 389-399 (2002).

38. Edinger, M. et al., CD4(+)CD25(+) regulatory T cells preserve graft-versus-tumor activity while inhibiting graft-versus-host disease after bone marrow transplantation. *Nature Medicine* **9**, 1144-1150 (2003).

39. Chen, W. et al., Conversion of Peripheral CD4+CD25- Naive T cells to CD4+CD25+ Regulatory T cells by TGF-beta Induction of Transcription Factor FoxP3. *J Exp.Med.* **198**, 1875-1886 (2003).

40. Fontenot, J. D. et al., Regulatory T cell lineage specification by the forkhead transcription factor FoxP3. *Immunity* **22**, 329-341 (2005).

41. Wang, Y. et al., The role of herpesvirus entry mediator as a negative regulator of T cell-mediated responses. *J Clin.Invest* **115**, 711-717 (2005).

Figure 1

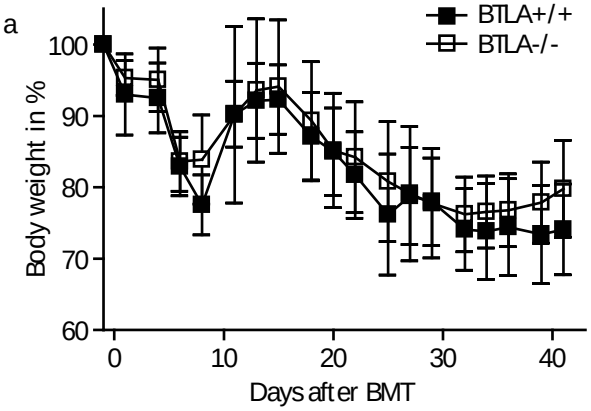
a
BTLA+/+
BTLA-/-
Body weight in %
Days after BMT

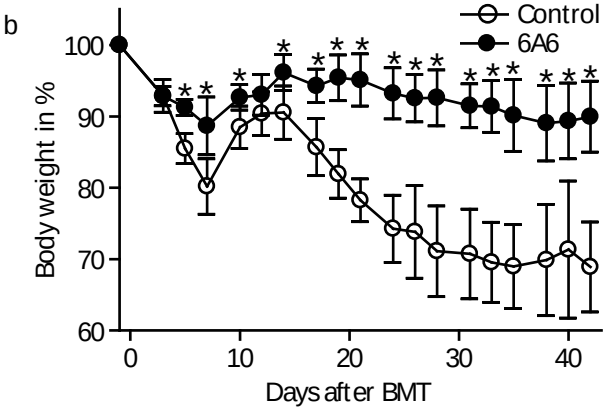
b
Control
6A6
Body weight in %
Days after BMT

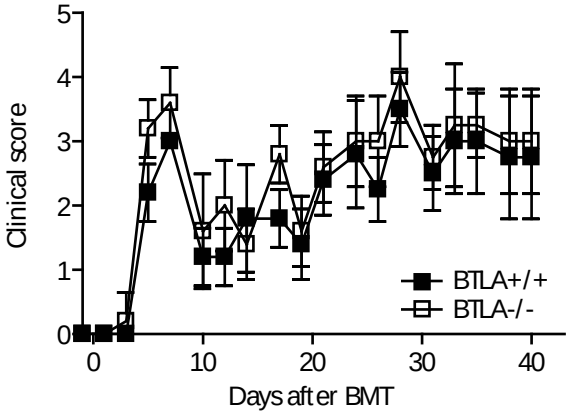
Clinical score
BTLA+/+
BTLA-/-
Days after BMT

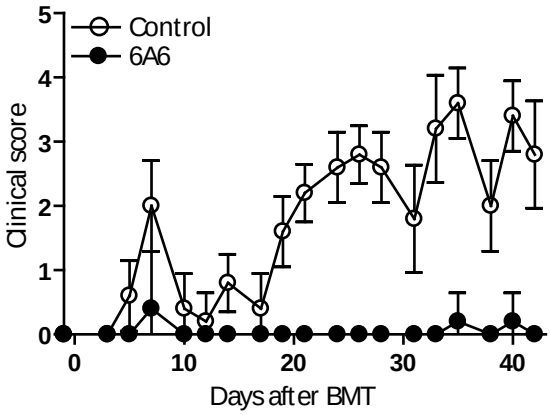
Control
6A6
Clinical score
Days after BMT

c

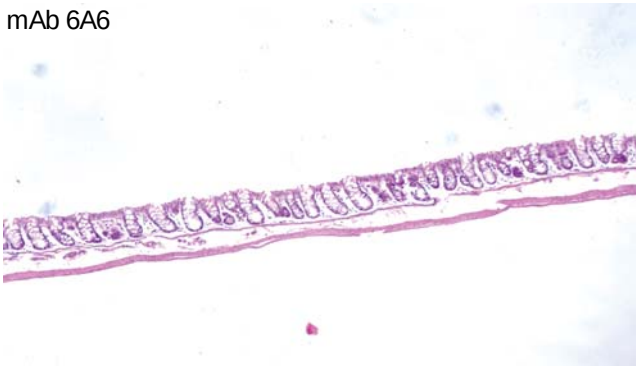
mAb 6A6

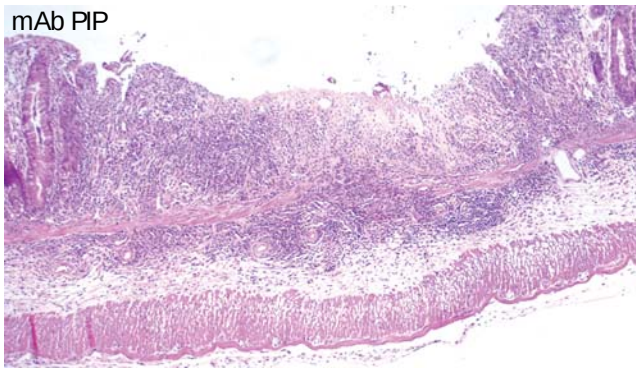
mAb PIP

Figure 2

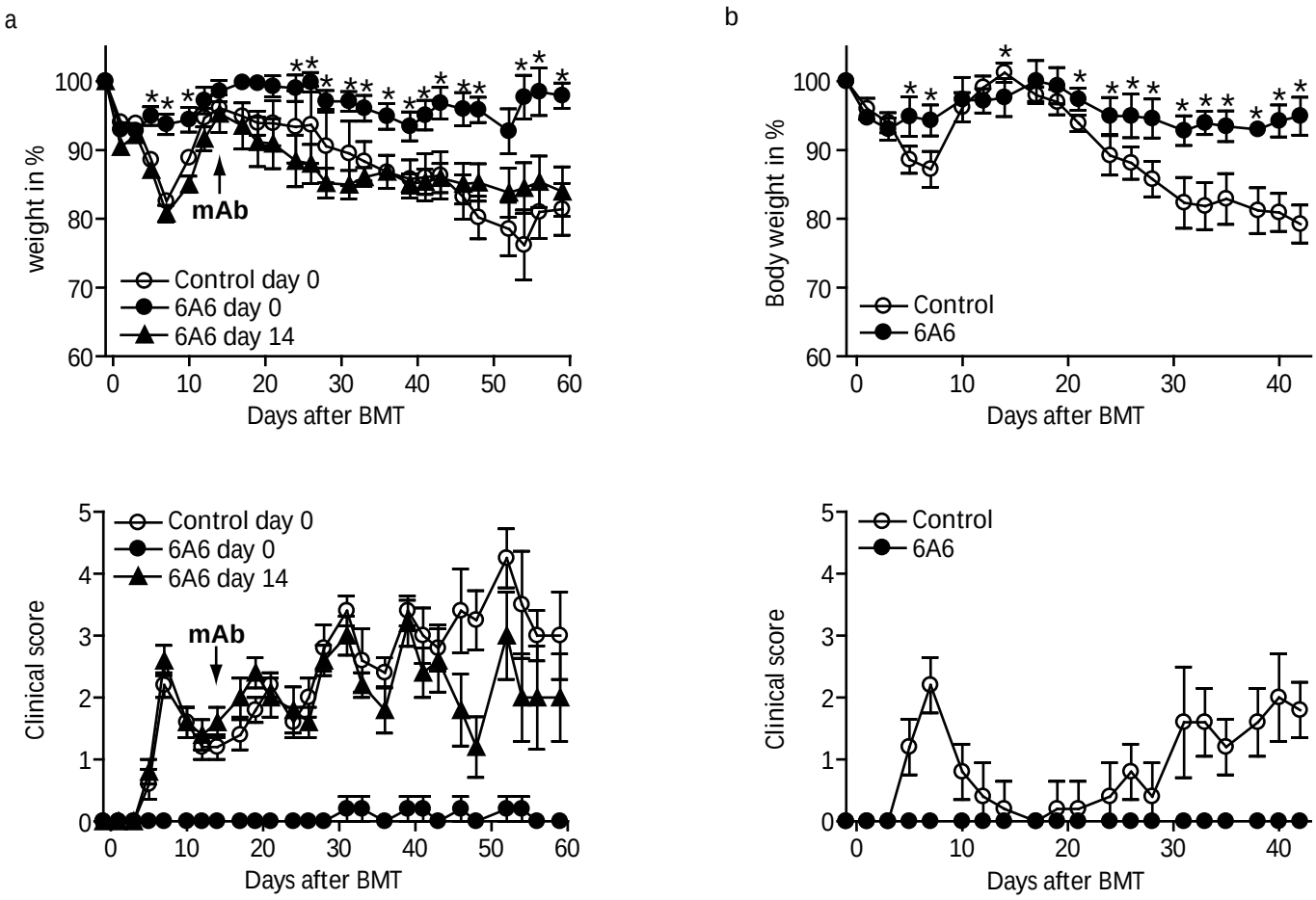
a
b
weight in %
Body weight in %
Days after BMT
mAb
Control day 0
6A6 day 0
6A6 day 14
Control
6A6
Clinical score

Figure 3

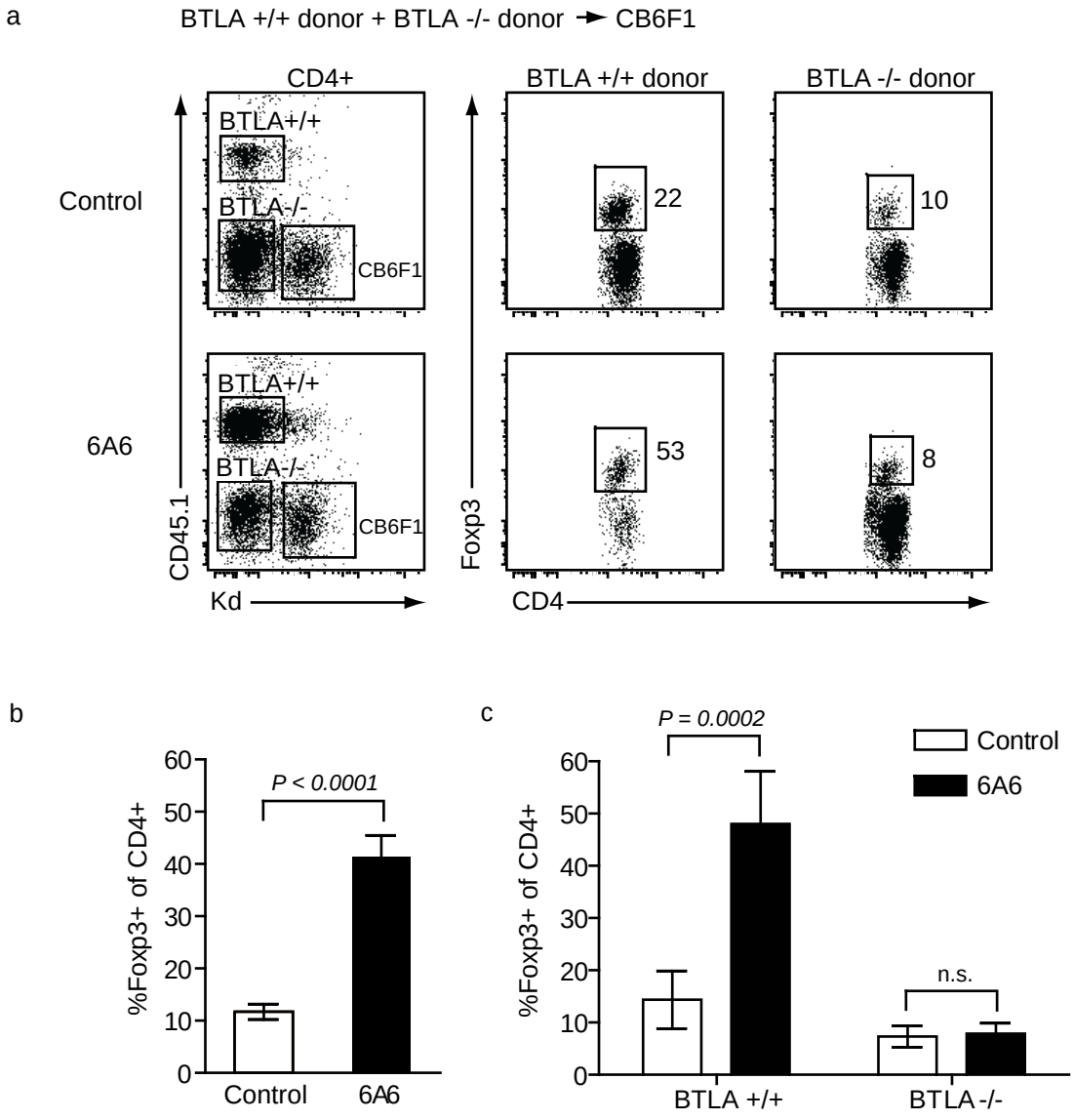
a
BTLA +/+ donor + BTLA -/- donor → CB6F1
CD4+
BTLA +/+ donor
BTLA -/- donor
Control
6A6
BTLA+/+
BTLA-/-
CB6F1
22
10
53
8
CD45.1
Kd
Foxp3
CD4
b
%Foxp3+ of CD4+
P < 0.0001
Control
6A6
c
P = 0.0002
Control
6A6
n.s.
BTLA +/+
BTLA -/-

Figure 4

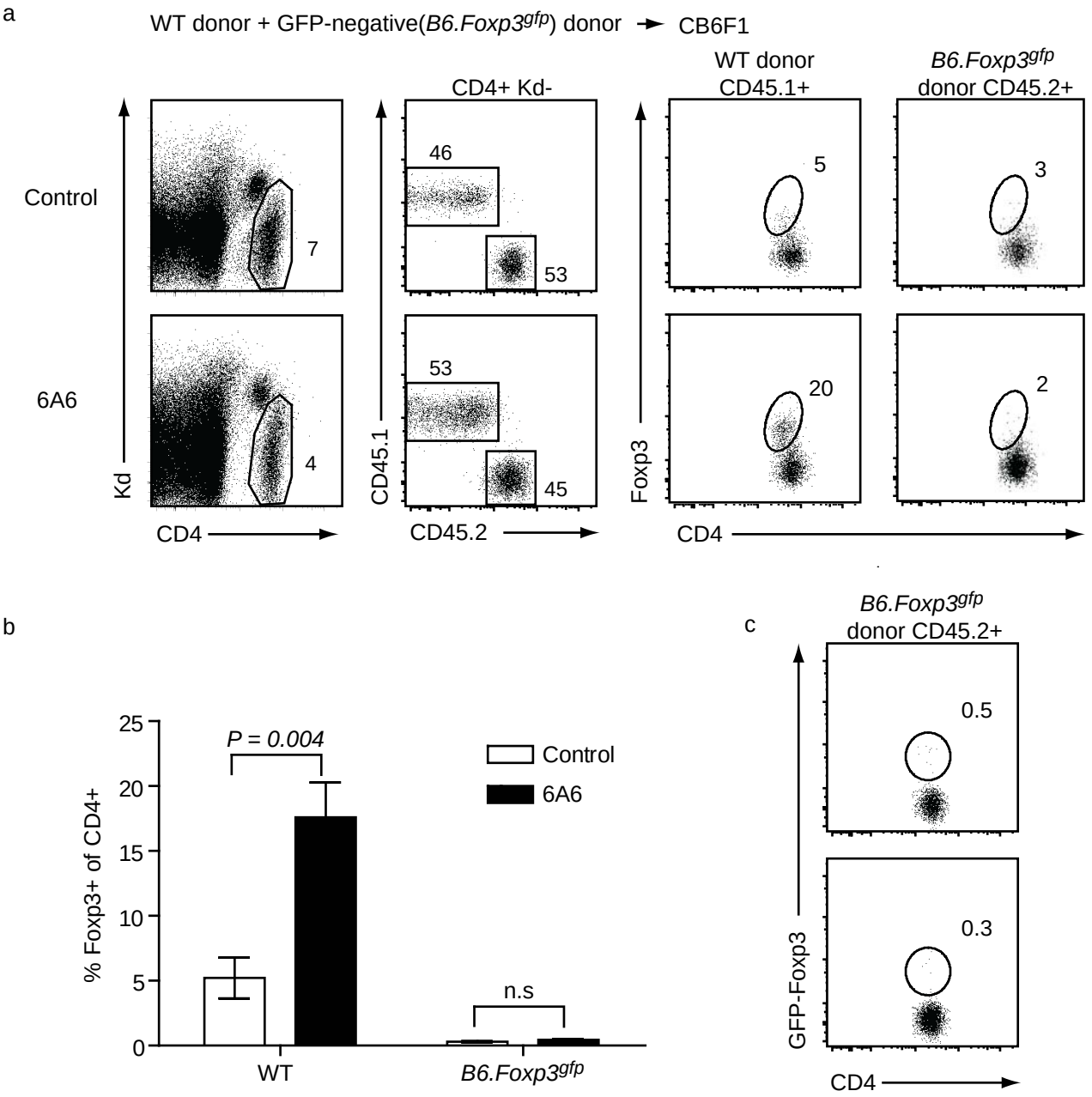
a
WT donor + GFP-negative(B6.Foxp3gfp) donor → CB6F1
CD4+ Kd-
WT donor CD45.1+
B6.Foxp3gfp donor CD45.2+
Control
6A6
Kd
CD4
7
4
46
53
53
45
CD45.1
CD45.2
5
20
3
2
Foxp3
CD4
b
P = 0.004
Control
6A6
% Foxp3+ of CD4+
25
20
15
10
5
0
n.s
WT
B6.Foxp3gfp
c
B6.Foxp3gfp donor CD45.2+
0.5
0.3
GFP-Foxp3
CD4

Supplemental Figure 1

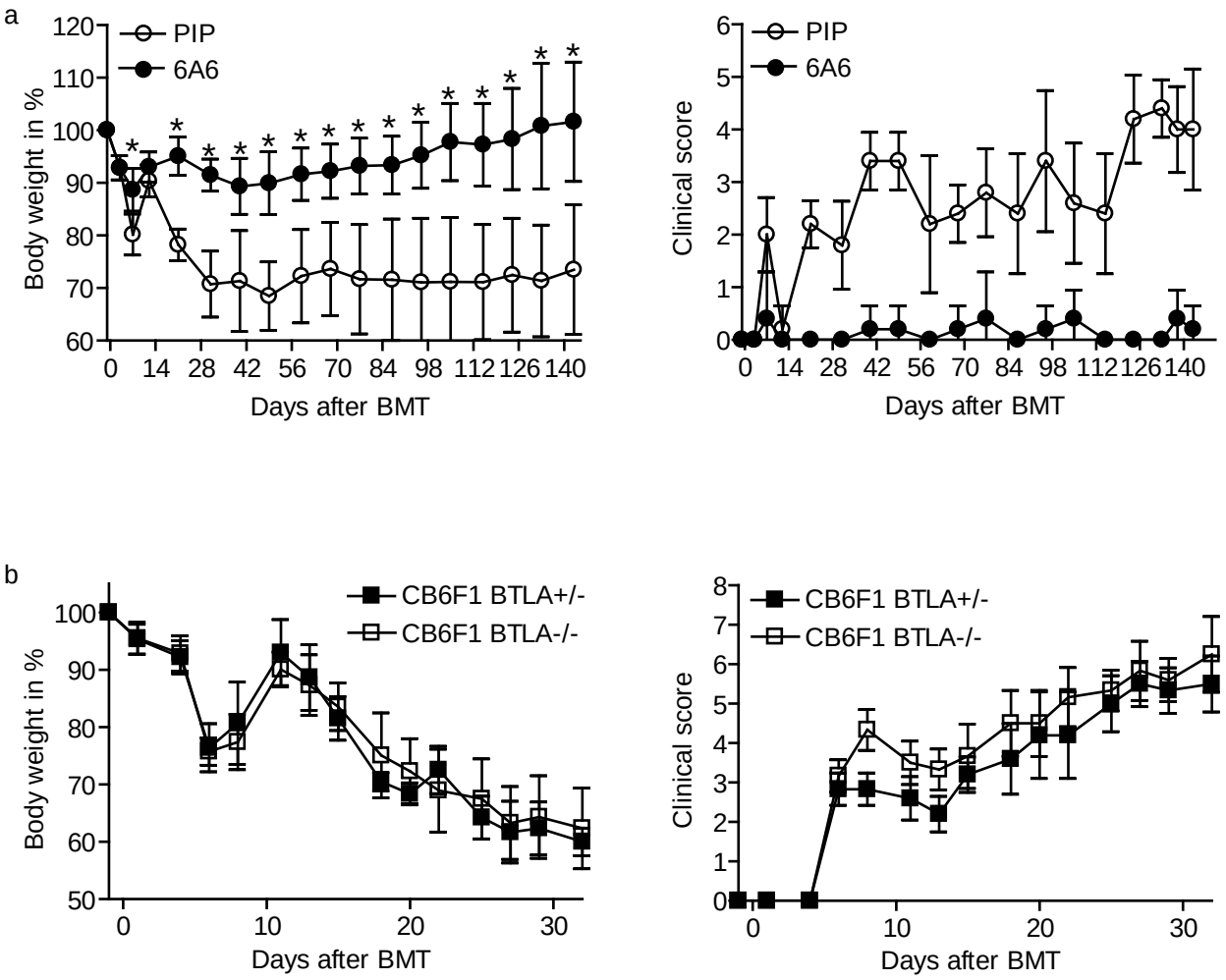

Supplemental Figure 2

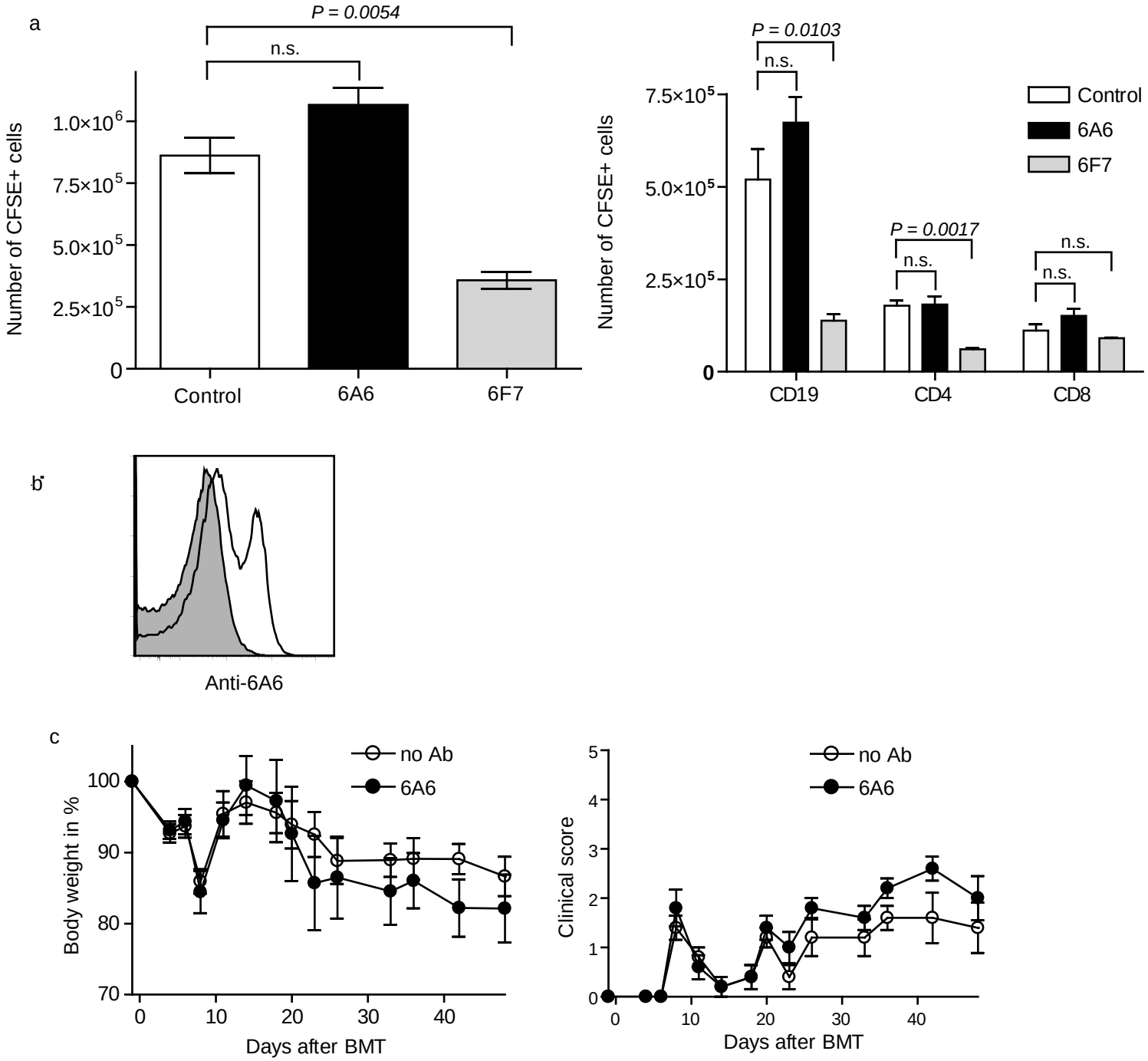

Supplemental Figure 3

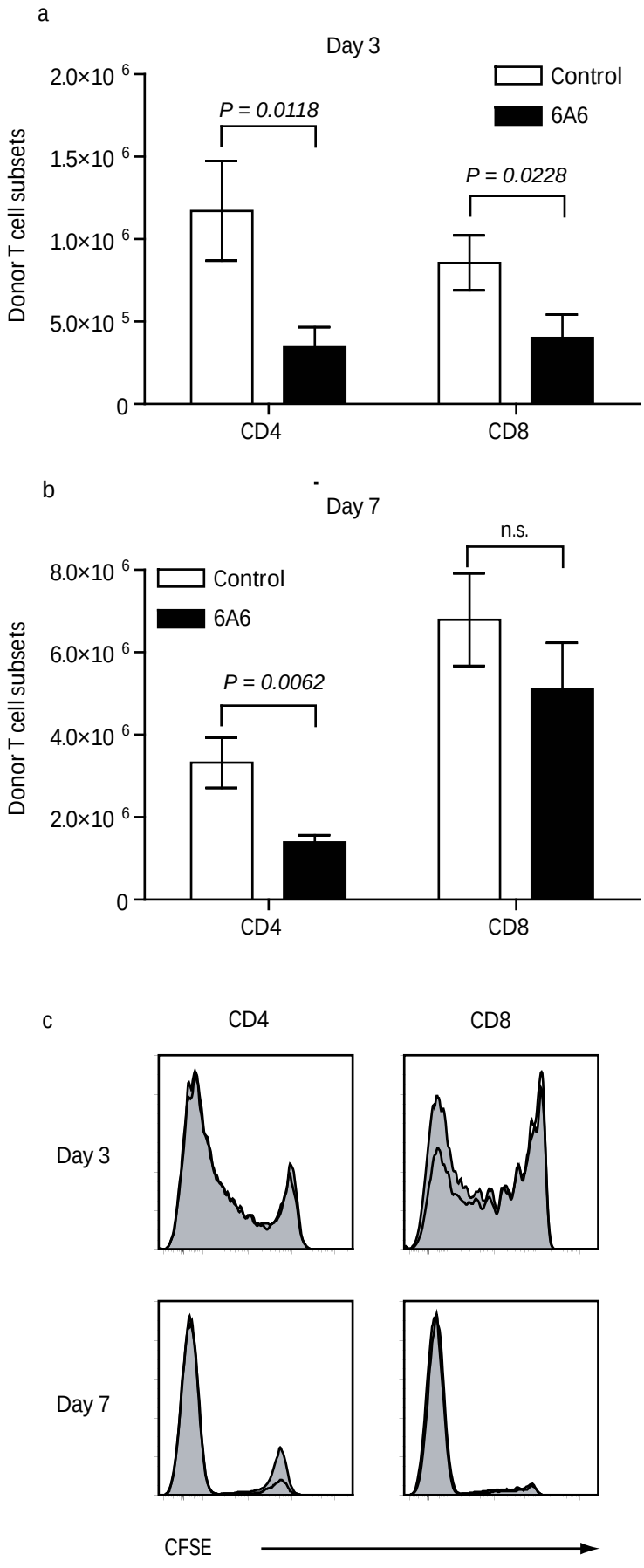

Supplemental Figure 4

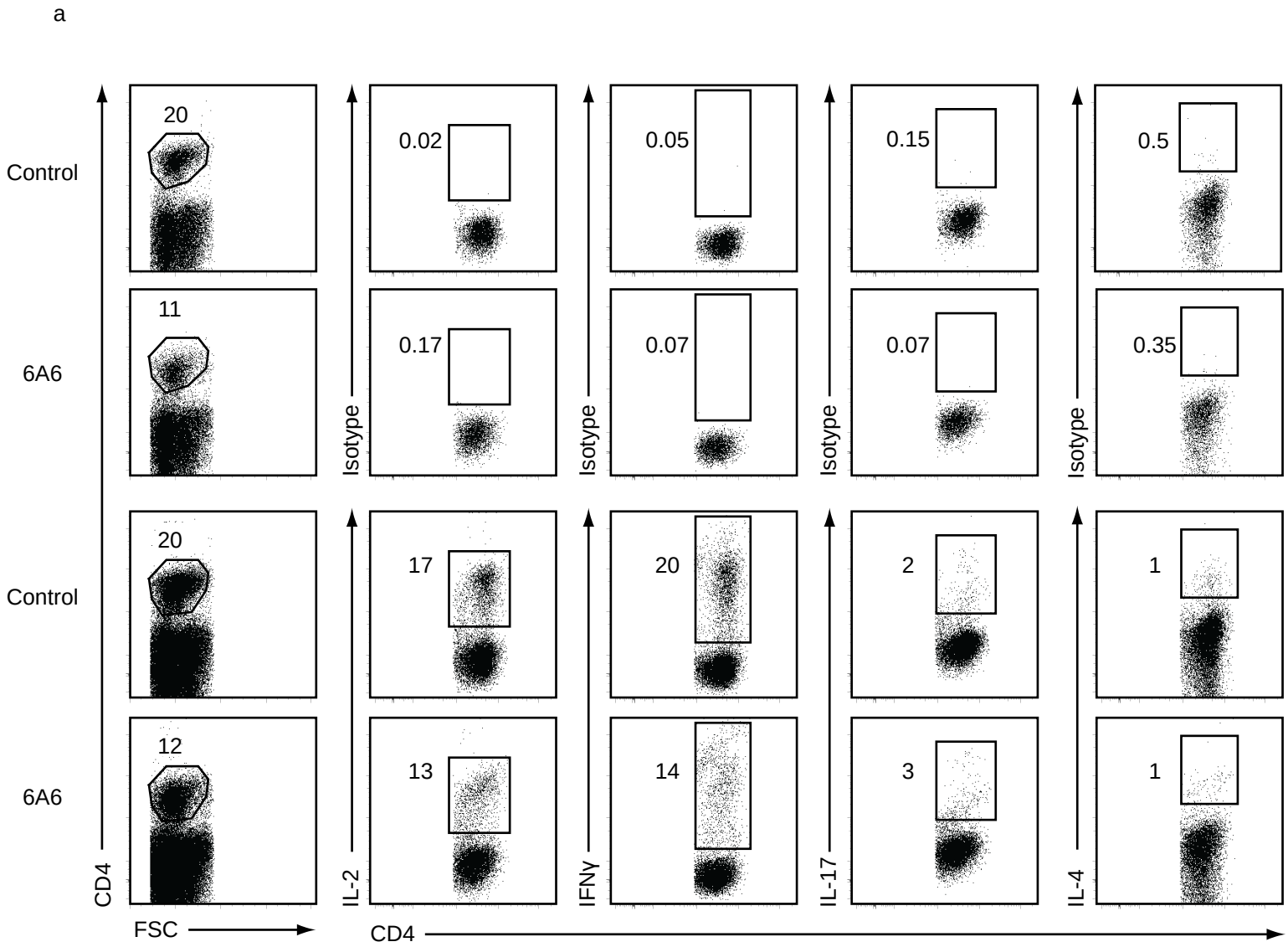


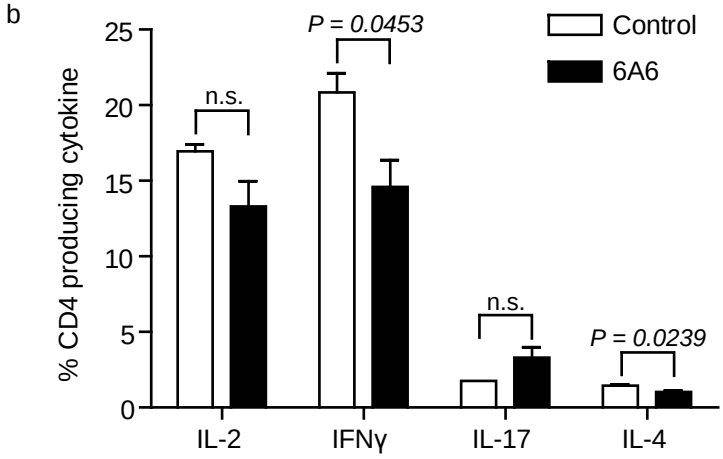

Supplemental Figure 5